

Durham Research Online

Deposited in DRO:

27 November 2019

Version of attached file:

Accepted Version

Peer-review status of attached file:

Peer-reviewed

Citation for published item:

Kabora, T.K. and Stump, D. and Wainwright, J (2020) 'How did that get there? understanding sediment transport and accumulation rates in agricultural landscapes using the ESTTraP agent-based model.', *Journal of archaeological science: reports.*, 29 . p. 102115.

Further information on publisher's website:

<https://doi.org/10.1016/j.jasrep.2019.102115>

Publisher's copyright statement:

© 2019 This manuscript version is made available under the CC-BY-NC-ND 4.0 license
<http://creativecommons.org/licenses/by-nc-nd/4.0/>

Additional information:

Use policy

The full-text may be used and/or reproduced, and given to third parties in any format or medium, without prior permission or charge, for personal research or study, educational, or not-for-profit purposes provided that:

- a full bibliographic reference is made to the original source
- a [link](#) is made to the metadata record in DRO
- the full-text is not changed in any way

The full-text must not be sold in any format or medium without the formal permission of the copyright holders.

Please consult the [full DRO policy](#) for further details.

Title: How did that get there? Understanding sediment transport and accumulation rates in agricultural landscapes using the ESTTraP agent-based model.

Authors: Kabora, T.K.^a (corresponding author), Stump, D.^b & Wainwright, J.^c

^a Department of Archaeology, University of York, The King's Manor
York, YO1 7EP, UK

^b Department of Archaeology, University of York, The King's Manor
York, YO1 7EP, UK

^c Department of Geography, Durham University, Lower Mountjoy
South Road, Durham, DH1 3LE, UK

Corresponding author's email and present address: tkkabora@gmail.com

Abstract

The 15th-18th century CE site of Engaruka in Tanzania is often described as primarily comprising drystone agricultural terraces, but it is now known that many of these former farming plots are not terraces *per se*, but are instead sediment traps. Stratigraphic excavations of these traps show that they were built by constructing low drystone walls adjacent to either natural or artificial water courses in order to capture fine alluvial sediments entrained within water flows. In the northern area of the site sediments were accumulated to a depth of up to 700 mm, while in one area in the south of the site over 2 m of deposits were accumulated over at least a 300 year period. The presence of sediment traps on archaeological sites allows investigations of the efficacy and sustainability of these structures over decadal to centennial timescales, since stratigraphic excavations can define the process of construction, and geoarchaeological analyses can explore changes within accumulated sediments over time. Although a combination of stratigraphy and absolute dating can discern the broad sequence and timing of sediment capture they cannot determine sediment-accumulation rates, and these techniques are too time consuming to be used to map the development of over 9 km² of sediment traps. The ESTTraP agent-based model provides these data by simulating sediment accumulation under different hydrological conditions. Four scenarios were simulated for a period of 100 years: constant water availability (SIM-01), seasonal variability (SIM-02), long-term climate variability (SIM-03), and vegetation-cover impact (SIM-04). The model

results suggest that the fields can be constructed over a short period of time, approximately 1 - 3 months per 6 × 6 m field, and that to construct a block of 90 fields covering 3,000 m² it would take between 8 to 13 years in periods of high water availability, and up to 27 years during prolonged dry periods. The results define the amount of time needed to construct individual fields, and suggest that farmers constructed blocks of fields concurrently rather than sequentially expanding across the landscape, and that the c. 10 km² area of sediment traps at Engaruka could have been constructed by a number of households working independently. The ESTTraP model presents an important resource in the assessment of sediment dynamics and patterns of field development, is relevant to a range of archaeological sites worldwide that include intentional or unintentional alluvial deposition, and has applications for modern landscape management.

Highlights

Technique for assessing long-term sustainability of sediment traps
Long-term patterns of sediment accumulation
Water availability the main constraint on sediment accumulation rates
Modelling of sediment accumulation helps refine site chronology
Landscape modifications can be achieved through house-hold level interventions

Keywords

Sediment transport
Sediment traps
Agent-based model
Engaruka
Water-management system
Sediment accumulation rates

1. Introduction

The construction of artificial sediment traps to create agricultural fields is a widespread practice (Mekonnen, et al., 2015), and is increasingly being recognised on archaeological sites. These include long-abandoned sites like Petra in Jordan (Beckers, et al., 2013) and extant farming systems in Ethiopia and Tunisia (Ferro-Vázquez, et al., 2017, Hill and Woodland, 2003), while other studies recognise

ancient sediment traps as exploitable legacies from previous periods of agricultural expansion or intensification (Giráldez, et al., 1988). Sediment traps can be built in a variety of ways and can perform one or more of several functions, including mitigating the impacts of soil erosion, stabilising sedimentation, increasing soil depth and soil-water storage capacity, reducing runoff or the velocity of channelled water, accumulating fine sediments for ease of tillage or root penetration, the incorporation of mineral or organic material beneficial to plant growth within agricultural plots, or to create flat areas for cultivation within valleys or at the base the slopes (Mekonnen, et al., 2015, Abedini, et al., 2012, Ran, et al., 2008). At the current case-study site of Engaruka in Tanzania, geochemical results suggest that the repeated accumulation of sediments within traps also avoided the salinization of soils (Lang and Stump, 2017); a common problem with prolonged irrigation, particularly in the tropics. The ability of archaeological research to identify these benefits, and to assess their efficacy over decadal to millennial scales, means it is well placed to contribute to assessments of agricultural sustainability (Fisher, 2019, Logan, et al., 2019) Since the construction of sediment traps leads to increases in the quantity of accumulated sediments over time, they provide an ideal case-study of how archaeological data-sets can be used to quantify change, and thus contribute to assessments of the costs and benefits of human-landscape modifications. In the current paper we employ agent-based modelling to explore the physical and environmental factors that influence the rates of sediment accumulation with sediment traps at Engaruka, and discuss why the rates of change are significant to questions of site chronology, resource use, agricultural management, social hierarchy and sustainability.

Within the archaeological literature sediment traps are sometimes classified as a form of runoff agriculture or as a runoff-terrace system (e.g. Beckers, et al., 2013, Evenari, et al., 1982), reflecting the fact that water-harvesting systems can unintentionally accumulate the sediments entrained within water flows, most obviously in the infilling of artificial reservoirs (Morrison, 2015). For some issues of relevance to agricultural management and sustainability, intentionality may not matter: the periodic addition of new sediments may have mitigated the effects of soil salinization at Engaruka, for example, but it cannot be concluded from this that the farmers who built these traps were aware of this effect. The question of intentional or unintentional accumulation of sediments remains important, however: the removal of

sediments inadvertently accumulated within irrigation canals, fields or reservoirs can be a time-consuming and labour intensive process (Sheridan, 2002) and may prompt their abandonment (Morrison, 2015) . At Engaruka, in contrast, the layout, method of construction, and physical extent of the area of sediment traps, strongly suggest that the famers who built the field system between the 15th and 18th centuries CE intended to exploit available river flows while deliberately capturing the sediments they carried, in the process creating c.9 km² of sediment traps up to 700 mm deep in the northern end of the site (Stump, 2016, Stump, 2006) , and accumulating sediments over 2 m deep towards the southern end of the field system (Lang and Stump, 2017).

The Engaruka system is of particular interest as excavations show that sediment trapping and accumulation was inherently tied to the construction and expansion of the system of drystone-bound fields bounded by drystone walls (Stump, 2006). Studies by Lang and Stump (2017) and Stump (2006) show that the drystone walls of the sediment- trap fields were not self-supporting and instead were supported by the accumulation of sediments behind the walls. This arrangement meant that wall courses were raised as the sediments accumulated in the sediment trap fields with farmers placing additional drystone wall courses over time that raised the height of the walls as the sediment depths increased. In addition, excavations (Stump, 2006) also showed that the sediment trap fields were built in a series of blocks with each block surrounded by a set of canals that transported the water and sediments to these fields (Fig. 2). Thus the rate of sediment accumulation influenced the construction of the drystone fields and the expansion of the field system across the landscape.

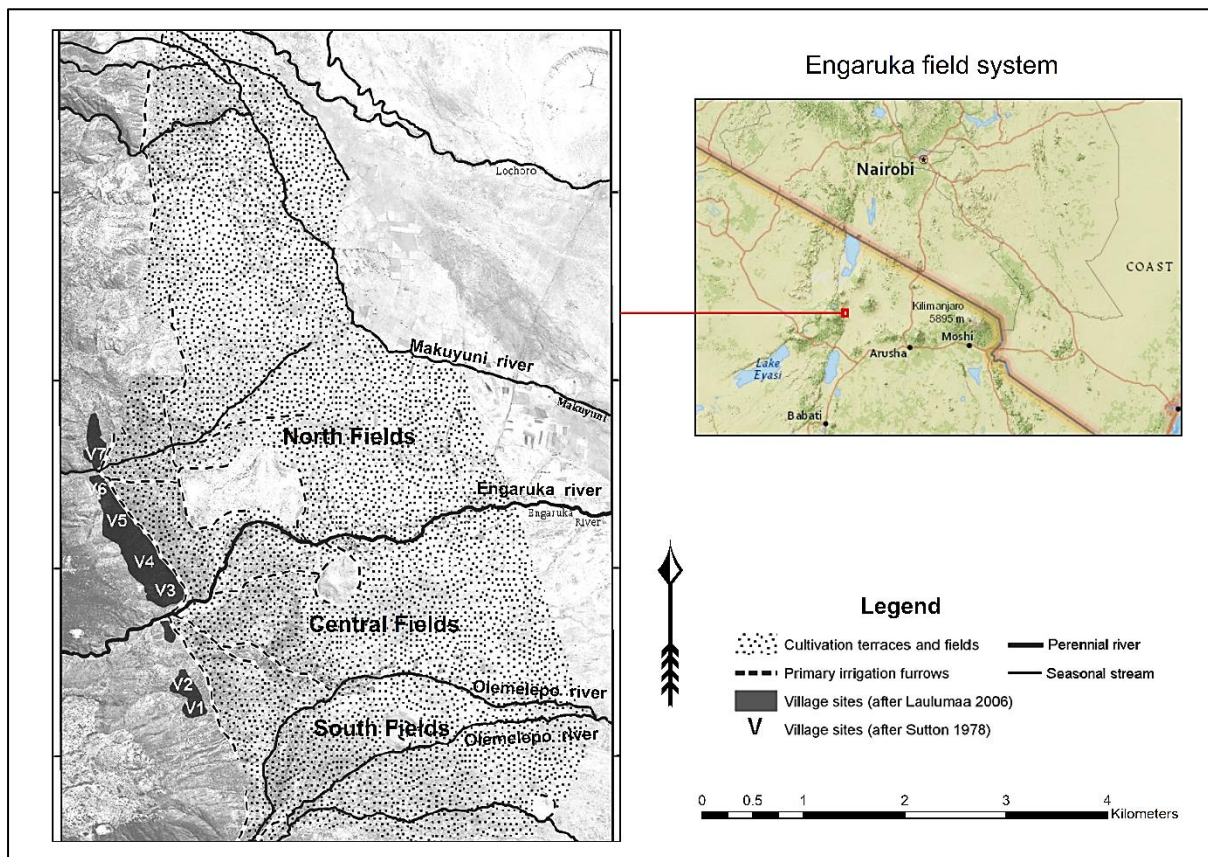
Although studies of archaeological stratigraphy can define the depth and extent of sediment accumulation, and can demonstrate broadly the sequence of sediment-trap construction, this approach provides little data on rates of sedimentation, and hence the rate, pattern and manner of the system's development. The aim of this study is thus to assess the effects of water- and sediment-transport dynamics on sediment accumulation and field development at Engaruka. In this paper we use evidence from archaeological excavations, field survey and aerial photographic data to create a simulated version of the North Fields area at Engaruka, and employ agent-based

modelling (ABM) techniques to simulate different hydrological scenarios based on data from modern irrigation at Engaruka and palaeoclimatic data from the region (Ryner, et al., 2008, Verschuren, et al., 2000).

ABM represents just one technique that can be used to approach this problem, with others including 'system dynamics' - a deterministic, top-down modelling approach that provides an aggregate view of the system's processes (Ding, et al., 2018, Martin and Schlüter, 2015) - and traditional discrete event simulation that employs a top-down, process-oriented modelling approach (Siebers, et al., 2010, Bonabeau, 2002). The choice to use ABM is to allow for the exploration of a variety of scenarios related to the hydrology and sediment processes, but is primarily intended to allow for future expansion of the model to incorporate more complex human-environment interactions such as farmer decision making. Whilst this paper is focused on an archaeological example, the techniques employed have the potential to contribute to studies of the efficacy and sustainability of sediment-trap systems in the modern world by providing information on the accumulation of sediments over centuries, rather than simply over the few years available to modern observational studies (Barton, 2016).

2. Study Area and Archaeological Background

Engaruka provides an opportunity to study sediment-transport and accumulation processes over long temporal scales which would otherwise be difficult in modern extant agricultural systems. The site is located in the East African Rift Valley, is centred at 2° 59' 20" S, 35° 57' 45" E, and the former field area slopes from west to east from c. 1000 m asl to c. 850 m asl (Fig. 1). The system of irrigated agricultural fields at Engaruka was abandoned by the 19th century CE, covers approximately 20 km², and comprises an extensive network of irrigation channels, stone-bound fields, agricultural terraces and sediment traps (Westerberg, et al., 2010, Stump, 2006, Sutton, 1978). The abandoned field system has been categorised into three distinct sections of the North, Central and South Fields (Sutton, 1998) (Fig. 1) based on differences in field construction, with the majority of the North Fields and parts of the South Fields constructed through periodic sediment capture and accumulation, while the Central fields were built by tilling the existing topsoil and removing stones from the field area (Lang and Stump, 2017, Stump, 2006).



172

173 Figure 1: Location of Engaruka and extent of the agricultural field system, showing
 174 river sources and village settlements (Laulumaa, 2006, Sutton, 1978). Source of
 175 regional map: National Geographic World Map (Esri, 2011). Copyright © Esri.

176

177 Detailed stratigraphic excavations (Stump, 2006) and a combination of stratigraphy,
 178 geochemistry and soil micromorphology (Lang and Stump, 2017) have demonstrated
 179 how sediments were accumulated. The results of excavations and surveys
 180 undertaken in the North Fields area of Engaruka in 2002-3, reported in Stump
 181 (2006), demonstrated that fields in this area were constructed by building a series of
 182 c. 6 × 6 m L-shaped drystone walls, with each new L-shaped wall forming a roughly
 183 square field by abutting earlier walls built in the same manner (Fig. 2b). The water
 184 and sediments supplied to this block of fields were transported from the main river
 185 Engaruka by the primary irrigation furrows (Fig. 1) which then branched off into the
 186 smaller canalised streams and irrigation canals (Fig 2a) that distributed water and
 187 sediments into the blocks of fields. The individual fields within the block are

interconnected by a series of smaller channels that allow distribution of water and sediment between the fields and excess runs off into the canalised stream (Fig 2c).

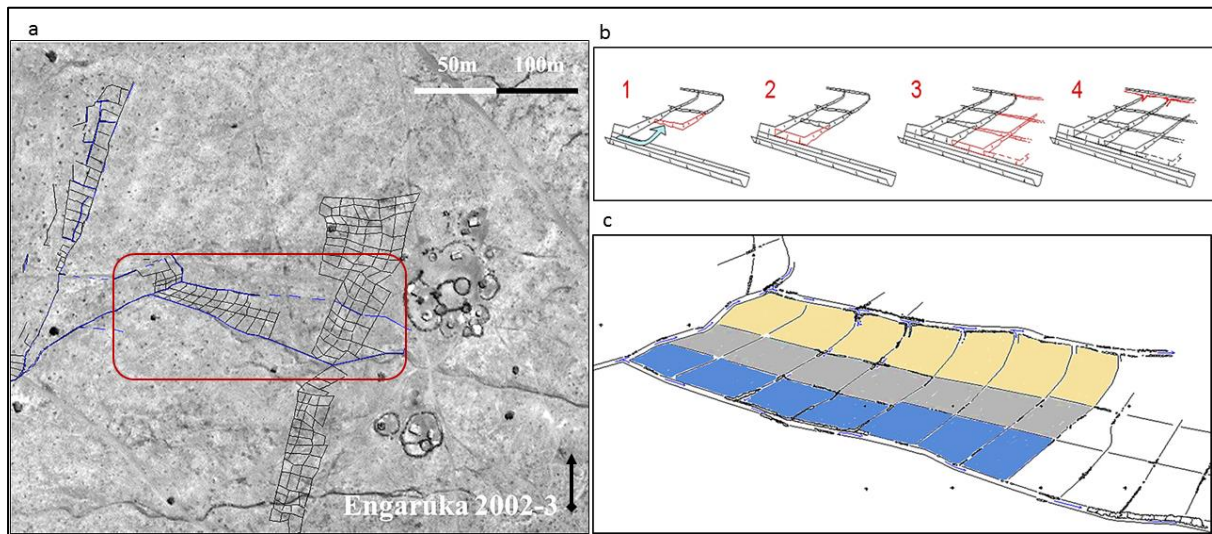


Figure 2: a) Location of the block of fields being modelled (within the red bounding box), the blue lines indicate the water channels and canals that surround a block of 6 x 6 m drystone-bound fields; b) Phases of field construction based on excavations of part of the North Fields (Stump, 2006); c) Plan of the group of sediment trap fields and associated water channels in the North Fields section of Engaruka used to simulate the field system in the ESTTraP model, based on excavations conducted by Stump (2006). Interpretation of stratigraphic data suggests that the fields were constructed consecutively from the upper fields (yellow) through the middle fields (grey) and down to the lower fields (blue), and from left to right (i.e. from upslope to downslope).

There are, however, limitations to these stratigraphic data that in turn limit our ability to employ them to address broader issues regarded the development and management of the agricultural system. The first of these - that these data demonstrate the sequence and manner of field construction but provide no information on the time it took to build an individual field or group of fields - has been highlighted already. A second limitation requires a little more explanation, and arises from the fact that it is often difficult or impossible to discern on purely stratigraphic grounds whether irrigation channels, canals or ditches were built in one construction episode or through successive phases of construction; an issue most commonly discussed in terms of identifying maintenance of structures or differentiating

maintenance from modification (Doolittle, 2015, Howard, 1993, Doolittle, 1984). To illustrate this in the case of Engaruka, note that the alluvial sediments captured within the fields could be delivered by water transported within the canalised stream (as shown in Fig. 2b, phase 1), with the stratigraphically later canal employed solely to deliver water for irrigation after these fields had been constructed (as shown in Fig. 2b, phase 4). Alternatively, it is equally possible that sediments were transported within the smaller irrigation canal, as suggested by observations and conversations with farmers in Konso, Ethiopia, who build analogous sediment traps by first diverting stream-flows along small canals (see Ferro-Vázquez, et al., 2017). Deciding between these two scenarios cannot be achieved based on the stratigraphic data alone, since the canal shown in Fig. 2b phase 4 could have been periodically extended: i.e. the stratigraphic evidence merely demonstrates that the ditch and drystone lining to this canal were inserted later than the field walls and captured sediments they truncate, not that the whole canal was built in a single construction episode. The construction sequence presented in Stump (2006) and summarised in Fig. 2b was thus based on the interpretative inference that collecting sediments entrained within comparatively small canals would take too long to be of practical benefit to farmers. Without data on possible sediment accumulation rates the interpretation of the sequence of field construction is merely an assumption.

The recognition that subtly different processes could produce the same sequence of field construction requires a method of investigating whether sediments were accumulated quickly during relatively large flood events or more slowly via the control of flows within small irrigation canals. One such approach is the use of ABM techniques since they can both explore the multitude of interacting hydrological and sedimentological factors involved and can investigate the effects of different scenarios such as changes to vegetation or climatic conditions. By modelling how water flowed through the irrigation channels, it is possible to assess how much entrained sediment could be transported, and therefore extrapolate the amount of sediment that can be accumulated and the rates at which these sediment traps could be constructed and expanded over time.

3. Materials and Methods

3.1 Engaruka Sediment Transport and Trapping (ESTTraP) Model Overview and Framework

The ESTTraP model is implemented in the NetLogo platform version 5.2.1 (Wilensky, 1999) and its documentation is based on the ODD+ protocol (Müller, et al., 2013, Grimm, et al., 2006). In this implementation of the model, a block of 90 individual stone-bound fields were modelled to understand the timescales and pattern of sediment accumulation given simulated scenarios of different environmental conditions. Using a georeferenced digital elevation model to build the model environment, the ASTER GDEM V2 (NASA_LP_DAAC, 2011) was resampled using the nearest neighbour interpolation technique from the original 30 m resolution to a resolution of 6 m to match the size of the stone-bound fields recorded from excavations within the North Fields (Stump, 2006). Each field within the model thus has a 6 x 6 m resolution (Fig. 2 and Fig.3), with sediment accumulation simulated for a block of 90 such fields covering approximately 3,000 m² of the c. 9 km² North Fields area of Engaruka (Fig. 1).

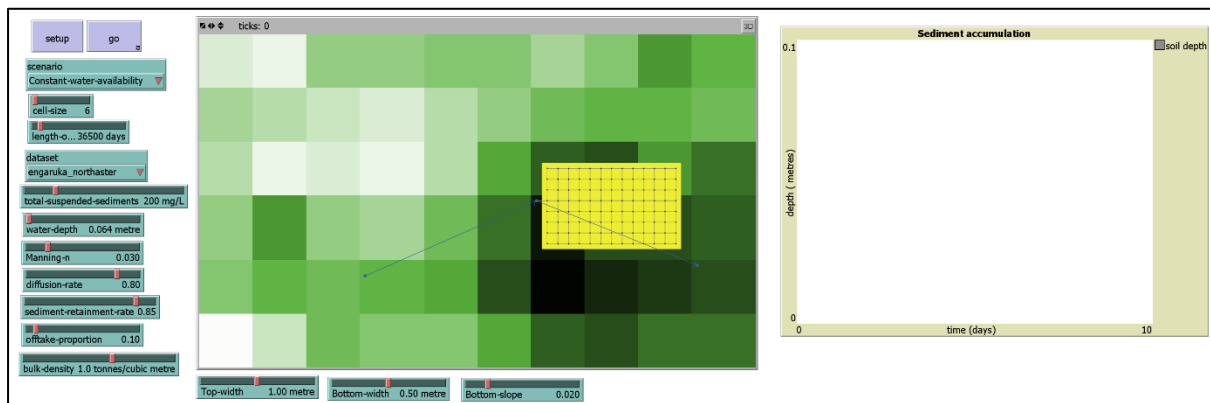


Figure 3: ESTTraP model interface showing the modelled block of fields (yellow) connected by a network of canals.

Excavation evidence shows that the process of accumulating sediments acted to level slight variations in slope of the pre-existing topography. This is clearest in the fields constructed adjacent to the canalised stream where up to 700mm of sediments were captured on their downslope side with as little as 100 mm towards their upslope extent, resulting in a wedge shape of captured sediments (Stump, 2006). This pattern of sediment accumulation allowed for sloping land to be levelled for improved

agricultural production. The sediment depth of 700 mm across the block of 90 fields therefore represents a maximal depth of accumulated deposits with the assumption that the fields are of equal dimensions and that the excavated examples are broadly representative of other fields in this area. For the purposes of the current modelling process we have therefore taken 350 mm as an average depth of sediment accumulation, i.e. approximately half of the maximal average depth of 700 mm to account for this wedge shape.

The hydrological and sediment-transport model is implemented through agents consisting of a network of nodes and directional links to represent the irrigation channels that transport water and sediments to the fields. The nodes contain information on the flow and sediment discharges along the system of canalised stream and irrigation channels based on the agent characteristics. The directed links that represent the irrigation channels distribute water and sediments from the canalised stream into the fields via nodes set within each 6 x 6 m field. At each model time step (representing a day) each node shares a percentage of its amount of sediments and water equally with its neighbours in the network of nodes. The nodes also retain a percentage of the sediments and water flows to represent sediment and diffusion loss incurred as these agents move along the network. Sediments and water flows terminate at the fields, where the nodes transfer these agents to the field patches as sediment discharge, which is then converted to represent sediment accumulation (Appendix A.3).

The model runs on a daily time step with 365 steps per year, and with data collected at each time step on the amount of sediment accumulated and changes in sediment depth. At each time step agents perform the following actions (which represent the sub-models of the ESTTraP ABM):

1) Generation of water flows: the estimation of flow rates and discharge from the irrigation channels is based on Manning's equation for open-channel continuous flows for trapezoidal channels (Robert, 2014, 31):

$$Q = \frac{k}{n} (R)^{\frac{2}{3}} \sqrt{S} A \quad (1)$$

Q represents water discharge ($\text{m}^3 \text{s}^{-1}$) from the irrigation channels, k is a dimensionless constant (=1 for SI units), n is the Manning's roughness coefficient; R

represents the hydraulic radius (m); S represents the slope of the channel (m m^{-1}), and A is the cross-sectional area of the channel (m^2). The water is then transported and distributed to the canals and fields. The dimensions of the canals are based on archaeological data from excavations (2006), where a canal top-width of 1.0 m and canal bottom-width of 0.5 m (Appendix A) are used to estimate the hydraulic radius and cross-sectional area of the canal. On the basis of excavated examples, the total depth of canals (as opposed to channels and canalised streams) rarely exceeds 300 mm, but water depths and hence the wetted perimeter of canals is more important factors than the maximum physical depth of a canal. Simulated water-depths (section 3.2 below), in conjunction with these dimensions, are thus used to determine discharge.

2) Sediment transport and discharge: sediments are transported by water in the irrigation channels, with the model focused on sediments transported in suspension and discharged into the fields based on the following relationship (Van Rijn, 1993):

$$Q_s = Y C_t Q \quad (2)$$

Q_s represents sediment discharge (tonnes day^{-1}) into the fields. Q represents water discharge (m^3s^{-1}), C_t is the daily total suspended sediment (mg L^{-1}) and Y is a conversion factor that converts $\text{m}^3 \text{s}^{-1}$ to $\text{m}^3 \text{day}^{-1}$ and mg L^{-1} to tonnes m^{-3} .

Entrainment and re-entrainment of sediments in the canals is considered to be minimal as the canals modelled are stone-lined and relatively smooth, and thus representing the daily sediment as a constant, average value is reasonable.

3) Sediment accumulation in the fields: sediments discharged into the field then accumulate as a function of the sediment discharge and the bulk density of the sediments, constrained by a soil compaction factor (van Rijn, 2013, Wilkinson, et al., 2006, 7):

$$\Delta H_i = \frac{\Delta S_{tot,i}}{f_i} \quad (3)$$

Where:

$$\Delta S_{tot,i} = \frac{Q_{s,i}}{BD} C \quad (4)$$

ΔH_i represents the depositional layer thickness (m), $\Delta S_{tot,i}$ represents the total sediment volume in a given stone-bound field i ($\text{m}^3 \text{ day}^{-1}$), f_i is the area of a given stone-bound field i (m^2), $Q_{s,i}$ is the sediment discharge within a given stone-bound field i (tonnes day^{-1}), BD is the bulk density of the soil (for clays such as at Engaruka, 1.0 – 1.6 tonnes m^{-3}) (McKenzie, et al., 2002, FAO, 2006, 51), and C is a consolidation/compaction rate of deposited sediment (1 /days).

The model design assumes 100% sediment trap efficiency, whereby all sediments discharged into the fields were captured and accumulated within those fields, which is not unreasonable given the geometry of the surface and stone walls. Total suspended sediments (TSS) were kept constant at 200 mg L^{-1} , and the data values for TSS of c. 200 mg L^{-1} and the water depth of 0.1 m were selected based on a hydrological study conducted in 2015 along a 4 km section of the Engaruka River (Fig. 1). These instrumental measurements are not unreasonable in the long term when reviewed in conjunction with CRUTS data (Harris, et al., 2014) on the rainfall and temperatures for the region and provide baseline approximations since the system is now abandoned. The choice of water depth is further supported by the results of the sensitivity analyses which found that water depths greater than 0.5 m would result in increased water discharge, which could potentially damage the channel walls by eroding their surfaces (Appendix B).

3.2 Model Simulations and Scenarios

Global sensitivity analysis (Thiele, et al., 2014, Saltelli, et al., 2008) was conducted on the model parameters for water depth, TSS and Manning's n to explore model behaviour and the influence of model parameters on outputs (Appendix B). The model was then implemented using a series of four scenarios to try to understand how the environmental factor of rainfall availability and variability, represented by water depth, would influence water and sediment discharge and thus sediment accumulation. The four scenarios simulated in the model are: SIM-01 Constant water availability, SIM-02 Seasonal variability, SIM-03 Long-term climate variability, and SIM-04 Vegetation cover impact. The scenarios modelled are about end-members, i.e. the diverse unimodal grain-size populations of sediments that are the result of different erosive processes (Seidel and Hlawitschka, 2015), and are intended to constrain sediment-transport rates rather than being realistic representations of the

compositional aspects of sediment-transport processes. The implementation of these four scenarios would help define the timescales involved in accumulating sediments within the field system. Simulations were run for a period of 100 years at a daily time-step to incorporate multi-decadal variability in climate conditions. Model uncertainty was assessed using Monte Carlo simulation of runs whereby the model scenarios were simulated over 100 replicated runs to estimate the distribution of model outputs.

SIM-01 Constant water availability: idealised conditions of constant water availability over time, which are intended to characterise an end-member of potential system behaviour, are represented by a constant water depth of 0.1 m based on observations of water-depths conducted during field survey along a 4 km stretch of the Engaruka River and modern irrigation channels in 2015.

SIM-02 Seasonal variability: the climate in Engaruka follows a bimodal rainfall pattern during a calendar year with two wet seasons interspersed with two dry seasons (Jones and Harris, 2008, Ryner, et al., 2008). The seasonal variability was simulated in the model by increasing and decreasing the constant water depth of 0.1 m by 20% to represent seasonal fluctuations in water availability. The 20% was an estimated range based on observations of the highest and lowest values of water depth from the observations made in 2015.

SIM-03 Long-term climate variability: in combination with seasonal variability, longer term climate variability is also evident within the East African region. Studies of palaeoclimatic proxies (Marchant, et al., 2018, e.g. Westerberg, et al., 2010, 305, Ryner, et al., 2008, Barker and Gasse, 2003, Verschuren, et al., 2000) suggest that over the last 1,100 years the East African region has experienced warm and wet climates interspersed with long periods of drought at a decadal scale. The longer-term variability was simulated by increasing or decreasing the average annual water depth and intra-annual seasonal variability by 20% over decadal scales to simulate long dry or wet periods, which means that in this simulation the baseline flows are shifted up and down by 20% at a decadal scale and within that seasonal variability increases and decreases by 20% of the decadal baselines .

SIM-04 Vegetation cover impact: in combination with seasonal variability, the vegetation cover of a landscape also influences water-discharge rates with runoff increasing by approximately 30% on bare ground as compared to areas with

vegetation cover (Lesschen, et al., 2009). One of the possible outcomes of reduced vegetation cover would be increased surface runoff during rainfall events which could possibly result in increased water depth and elevated levels of entrained sediments in the channels.

The scenarios modelled are intended to explore how the differences in water availability over time (which is a factor of seasonal and long-term climate fluctuations and vegetation cover) influenced sediment accumulation within the sediment trap fields and thus field construction and expansion.

4. Results

Results of the sensitivity analyses show that sediment discharge can be interpolated from water discharge and that the model simulates this function as expected, such that as water discharge increases sediment discharge also increases. Sediment discharge is a linear function of water and TSS, and increases in the water depth values would therefore result in increases in the sediment discharged and therefore the accumulation rates in the fields (Appendix B). This approximation has implications for the results of the scenarios modelled in that the sediment discharge and consequent accumulation would be affected by the water depths simulated to represent the variability in water availability due to climate conditions. Relative to the variation of the model parameters, the uncertainty analyses show that the scenarios for climate variations that would result in variations in water availability play a role in sediment accumulation (Appendix B).

The results of the model simulations provide information on the amount of time and rates at which sediments accumulate within the entire block of 90 fields. The four scenarios of constant water availability (SIM-01), seasonal variability (SIM-02), long-term climate variability (SIM-03), and vegetation cover impact (SIM-04) were simulated for a period of 100 years at a daily time-step to see how long it would take to accumulate sediments to the observed depths of 350 mm (Fig. 4). It would therefore take a shorter time to accumulate sediments, with sediments accumulating to a depth of 350 mm across the 3,000 m² block of 90 fields after 8 years for conditions modelled in SIM-01 and SIM-04, and 13 years for SIM-02 and SIM-03 (Fig. 4). Given that it would take 8 – 13 years to accumulate sediments across the

block of fields, it would take approximately 1 – 2 months to build each 6 x 6 m field individually. This range of estimates from the model end-members provides a maximum and minimum time scale for the development of the fields.

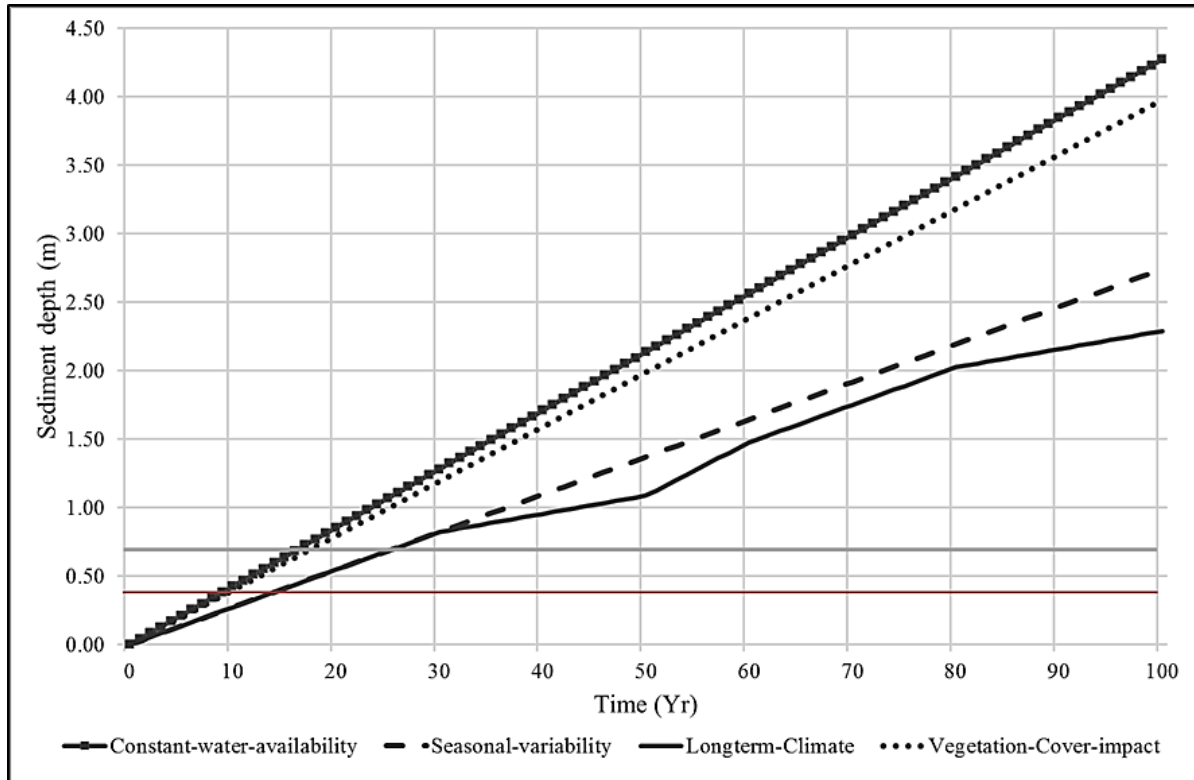


Figure 4: Mean annual cumulative sediment depth (metres) for a block of 90, 6 × 6 metre stone-bound fields based on simulations for four scenarios of constant water availability (SIM-01), seasonal variability (SIM-02), long-term climate variability (SIM-03), and vegetation cover impact (SIM-04) over a period of 100 years. The horizontal grey line highlights the sediment depth of 700 mm and the red line highlights sediment depths of 350 mm corresponding to those observed from the archaeological excavations.

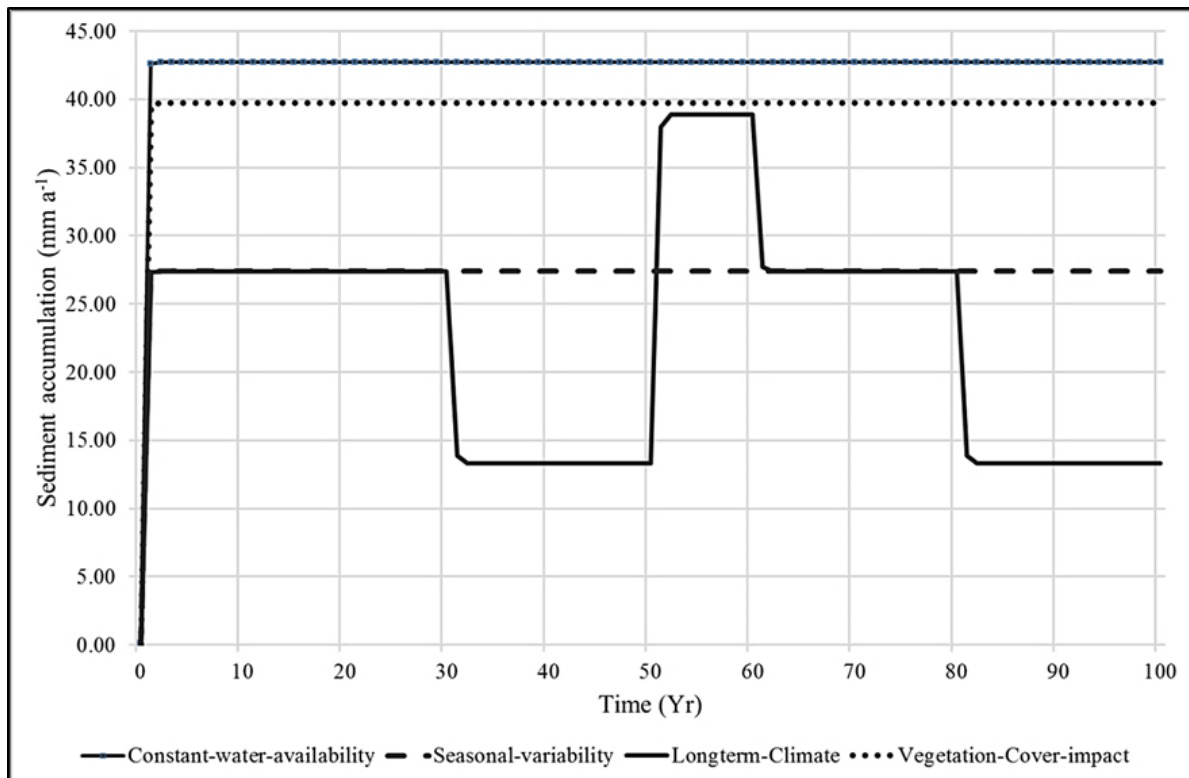


Figure 5: Mean annual sediment accumulation rates (mm a^{-1}) modelled for the four scenarios of constant water availability (SIM-01), seasonal variability (SIM-02), long-term climate variability (SIM-03), and vegetation cover impact (SIM-04) for a block of 90 fields over a period of 100 years.

Looking at the average annual rates of sediment accumulation for a block of 90 fields (Fig. 5), SIM-01 had the highest rates at 42 mm a^{-1} , followed by SIM-04 at 39 mm a^{-1} and SIM-02 at 27 mm a^{-1} . Longer term variations in climate account for the fluctuations in sediment accumulation rates seen in SIM-03, ranging from 38 mm a^{-1} during the much wetter periods, to as low as 13 mm a^{-1} during the periods simulated for extreme dry conditions, and an average of 22 mm a^{-1} over the 100 years. This lower mean annual sediment accumulation rate of 22 mm a^{-1} means that it could have taken 16 years for sediment depths to reach 350 mm across the $3,000 \text{ m}^2$ block of 90 fields. The prolonged dry conditions simulated in SIM-03 were set to have a minimum water depth that would simulate low water availability but not the complete absence of water. This scenario is based on evidence that the perennial Engaruka River was one of the water sources for the irrigation channels in the North Fields (Stump, 2006, Sutton, 1998), meaning that water supply to the fields would have still been possible but the amount of water in the channels would most probably have been greatly reduced.

Although the annual sediment accumulation rates presented in Fig. 5 appear to be constant when averaged out for each year; these rates do not reflect seasonal fluctuations in water availability that would affect sediment discharge and accumulation within the fields. The influence of seasonal variability on sediment accumulation was therefore explored further to see how these intra-annual/daily fluctuations influence sediment accumulation rates (Fig. 6 and Fig. 7). It should be noted that there is no simulation for intra-daily variability as the model assumes shorter timescale variability averages out for the purposes of this study.

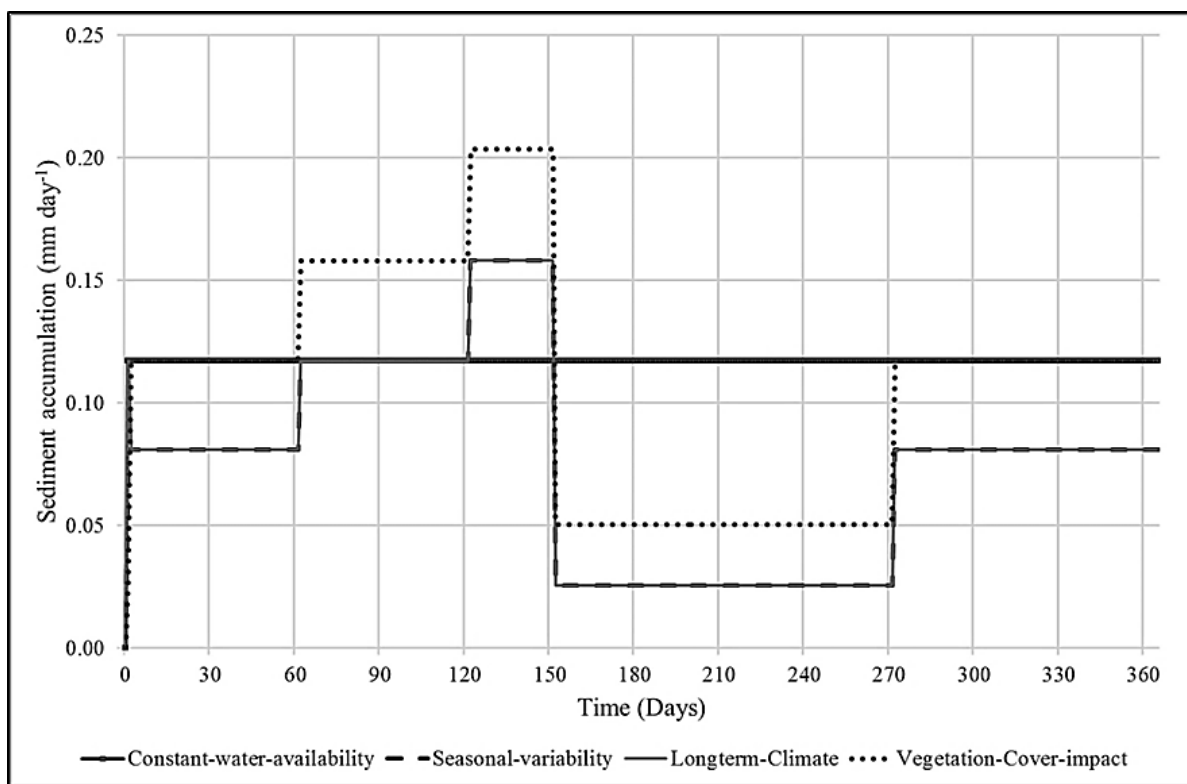
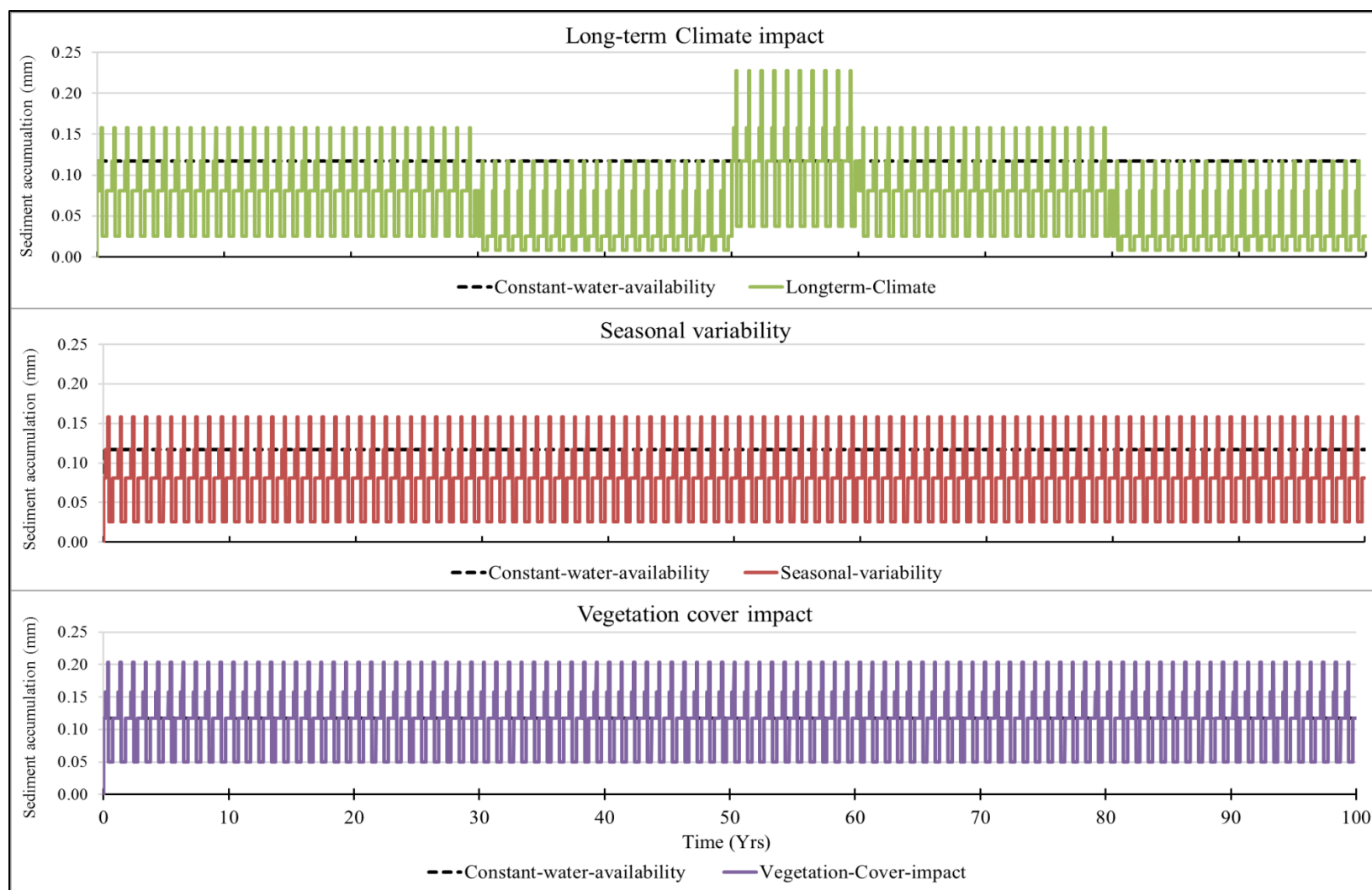


Figure 6: Intra-annual/daily sediment accumulation rates (mm day^{-1}) show the variations in sediment accumulation over a one year period i.e. Year 1 of the model for scenarios of constant water availability (SIM-01), seasonal variability (SIM-02), long-term climate variability (SIM-03), and vegetation cover impact (SIM-04).

As shown in Fig. 6, for SIM-02 and SIM-03 the average daily sediment accumulation rates ranged from 0.03 mm day^{-1} during the dry seasons to 0.16 mm day^{-1} during the rainy seasons, while the daily rates for SIM-04 ranged from 0.05 mm day^{-1} in the dry season to 0.20 mm day^{-1} in the rainy seasons. This result is in contrast to SIM-01 where the daily rates throughout the year were constant at 0.12 mm day^{-1} .

Simulations for long-term climate variability combined with seasonality (SIM-03) had the greatest impact on the sediment accumulation within the fields, with scenarios suggesting that it would take 13 years to accumulate 350 mm of sediments across the block of 90 fields (Fig. 4). However, over the longer timescales of the 100-year period (Fig. 7) these seasonal fluctuations varied further based on extremes of drought or wetter conditions. When extreme dry conditions were simulated between Year 30 - 50 and Year 80 – 100, these sediment accumulation rates dropped to 0.01 mm day⁻¹ during the dry seasons and were highest at 0.12 mm day⁻¹ during the rainy seasons. In the wetter periods simulated between Year 50 - 60, these sediment-accumulation rates were 0.04 mm day⁻¹ during the dry seasons and rose to 0.23 mm day⁻¹ during the rainy seasons (Fig. 7). These periods of extreme weather had a marked effect on sediment depth within the block of fields with the average depth at 2.30 m after the 100-year period, the lowest of all the simulations. The results of these climate-variability scenarios mean that if farmers attempted to accumulate sufficient sediments to fill these fields to the 350 mm depths observed archaeologically during a comparatively wet period the fields could be filled in 9 years, but attempts to do the same during the conditions that prevailed during the dry period would take 27 years.



507

508 Figure 7: Daily sediment accumulation rates (mm day⁻¹) simulated for scenarios of constant water availability (SIM-01), seasonal variability
 509 (SIM-02), long-term climate variability (SIM- 03), and vegetation cover impact (SIM-04) over a period of 100 years.

The low or no vegetation cover in the catchment simulated for in SIM-04 would result in higher surface runoff and water influx into the channels. This would then result in higher discharge rates and thus higher sediment accumulation rates within the fields such that SIM-04 resulted in high annual sediment accumulation rates at 39 mm a⁻¹ (Fig. 5). The block of fields took an average of 9 years to accumulate sediments to a depth of 350 mm across the c. 3,000 m² block of 90 fields. These high rates of sediment accumulation could also be seen in the daily rates for SIM-04, ranging from 0.05 mm day⁻¹ in the dry season to 0.12 - 0.16 mm day⁻¹ and then rising to 0.20 mm day⁻¹ in the rainy seasons (Fig. 6 and Fig. 7). SIM-04 presents a case that takes into consideration the removal of vegetation cover from the upslope catchment areas that could result in increased surface runoff in the short term. In addition, the possible removal of forest vegetation cover on the hillslopes upstream of the agricultural fields is likely to have affected water availability over the longer-term in both dry and rainy seasons, with the loss of vegetation and soil reducing the water holding capacity within the upland river catchments.

5. Water availability, sediment accumulation and field development

The four scenarios influencing water availability explored in the model present important steps in understanding the temporal scales and patterns of field development that resulted in the expansion of the Engaruka water-management system. As discussed in Section 1 and 2 above, the excavations of the site show that the construction of the drystone-bound fields was tied to sediment accumulation. The farmers would lay a few courses of the drystone walls and as the sediments accumulated behind these drystone walls the farmers could add further courses when needed, thus construction of the wall courses and the sediment trap fields were tied to the rate of sediment accumulation. The scenarios discussed above point to the influence of variability in water availability on the construction and development of a block of fields and the timescales involved. This variability relates to both seasonal and long-term climate changes that affected the east African region (Marchant, et al., 2018); and by focusing on specific aspects of water availability, we can use this information to understand the patterns of sediment accumulation and field construction that influenced the development of the Engaruka system. Understanding the impacts of seasonality, climate variability and vegetation cover on the availability of water and sediment accumulation helps support interpretations of

the archaeological evidence by providing additional data to refine stratigraphic interpretations of the timelines and patterns involved in the development of the field systems.

The block of 90 fields simulated in the model took between 8 to 13 years, and up to 27 years during prolonged dry conditions, to accumulate sediments to a depth of 350 mm, given differing scenarios of water availability for sediment transport. At a finer resolution it would take individual 6 x 6 m fields between 1 - 2 months when flows are occurring to accumulate sediments to depths of 350 mm and the farmers would be able to add one or two courses to the drystone walls with the sediments accumulating behind these wall courses. This means that farmers can construct individual fields within a field block over a period of a single cropping/growing season and continue to add wall courses and expand field construction across the block of fields. The timescales presented by this model are best estimates of average conditions for sediment accumulation and field construction. The model results suggest that the fields could have been developed by utilising low flows of water in irrigation canals to transport and accumulate sediments in small fields over successive seasons, and thus do not require the larger flooding events from overbanking or diverted streams envisaged by Stump (2006).

The amount of time it would take to accumulate 350 mm of sediments within a block of fields also points to concurrent construction of multiple blocks of fields across the entire Northern Fields areas rather than the consecutive construction of field blocks; an interpretation suggested by Stump (2006) on the basis of stratigraphic data and the interpretation of field layouts in relation to water courses, but one which remained speculative without approximations of sediment accumulation rates. Given model results suggesting 8 - 13 years to construct a block of 90 fields covering 3,000 m², it would take between 24,000 - 39,000 years to construct the fields across the entire 9 km² of the North Fields if the field blocks were constructed sequentially. These time scales are clearly far beyond the time periods in which Engaruka was in use. Indeed, the North Fields area only forms part of the entire 20 km² field system, with accumulated sediment depths in the South Field area up to 2.0 m deep (Lang and Stump, 2017), making it unlikely that the society in the Engarukan system widely relied on sequential field construction. If the ESTTraP model results hold true for

real-world scenarios, multiple blocks of fields must have been constructed concurrently across the North Field sections, and it is possible that the North Field and South Fields areas of the site were also constructed simultaneously. This interpretation in turn has implications for discussions of social hierarchy and resource management, as it suggests individual farmers, households or extended families (such as clans) could have built the extensive field remains and irrigation network without the need for central control or long-term planning, with each block of fields constructed and managed by a small group of individuals.

The ESTTraP model demonstrates the utility of agent-based modelling to assess the sediment transport dynamics and their influence on sediment accumulation and patterns of field construction. For example, although the results presented here suggest that farmers could utilise low flows of water to transport and accumulate sediments in the small individual 6 x 6 m plots evidenced in the North Fields, it is possible that much higher flows were employed to accumulate sediments quickly in the much larger fields located towards the south of the site (see Lang and Stump, 2017). This manipulation of the amounts of water flowing would influence not only the spatial scales but the temporal scales for the development of the field system as well as the choice of consecutive or concurrent field construction. However, there would nevertheless be limitations to this where diversion of water and sediment to multiple field blocks would limit the flow available to each plot. The construction of field blocks simultaneously would thus require water resources to be shared between the groups constructing each new block or irrigating existing plots, which would have further implications on water availability and the attendant water and sediment discharge capacity. This would also raise questions on the management of these water resources as issues of competition for water resources may arise among farmers, particularly when water flows are low during extended dry periods. These aspects of water sharing and competition are being further explored in versions of the ABM that assess the effect of concurrent field construction and which incorporates human agents within the simulated landscape.

6. Conclusions

The ESTTraP model demonstrates an ability to model sediment accumulation rates at the abandoned agricultural site of Engaruka, Tanzania, and given reasonable

model parameter approximations shows that blocks of fields at Engaruka are likely to have been constructed concurrently across the field system rather than sequentially. This conclusion substantially refines previous interpretations of stratigraphic evidence, showing that comparatively low water flows are sufficient to transport sediments that can be captured to create agricultural plots, and thus refutes an earlier interpretation of the stratigraphy of the field system (Stump 2006) that assumed the depths and extent of sediment capture required periodic or controlled flooding events. Field construction could occur over short periods with a single 6 × 6 m field taking 1-2 months and a block of 90 fields taking 8 -13 years given constant water flows of as little as 100 mm deep within canals with basal widths of 0.5m.

Moreover, the results have the potential to be combined with direct dating evidence of fields to refine the site's chronology of construction, and with better dating could be used to relate periods of field construction to palaeoclimatic evidence of changing rainfall regimes. The results of this model thus support arguments by Stump (2016) and Wainwright (2008) on the relevance of combining agent-based models with archaeological data for improved stratigraphic interpretations. The model results support archaeological interpretations where little additional information about the system is available such as direct evidence of water availability and rates of sediment accumulation and field expansion, making this model particularly relevant to other sites and studies for which little or no direct dating evidence is available. The results of these model scenarios would be of particular interest in understanding how other similar agricultural systems developed while taking into consideration the effects of long term climate on water availability.

Although tailored to a specific archaeological case-study, understanding the rates and patterns of field construction not only has a bearing for the abandoned agricultural site at Engaruka but is of relevance for any archaeological study involving the deliberate or unintended accumulation of alluvial sediments, including the siltation of basins or reservoirs, or the accumulation of sediments within run-off irrigation systems. Even further, knowing the rates and patterns of sedimentation is valuable in estimating alluviation in non-archaeological sites such as modern irrigation systems, whilst the ability to model these process over centennial timescales can aid in the assessment of the legacies of previous land-use and help

examine the future sustainability of modern land-use systems. The ESTTraP model thus presents an important resource in the assessment of sediment dynamics and patterns of field development at Engaruka as presented here, but can also be adapted for other archaeological sites and has further applications for modern irrigation systems and future landscape management.

Appendices

Appendix A: Model Overview

A.1 Model Assumptions

The ESTTraP agent-based model was constructed to perform a series of simulations to understand the temporal and spatial patterns for the transport and accumulation of sediments within a section of the stone-bound fields in the Engarukan water-management system. This model focuses exclusively on the physical processes of sediment transport and accumulation within a section of the stone-bound fields. The research presented here introduces a model that simulates water flows and sediment transport through a small section of the canal systems and through a c. 3,000 m² block of fields in the North Fields section of the site in order to demonstrate the core features of sediment accumulation. The model omits more complex landscape-scale elements: rainfall and surface runoff and erosive processes, as well as site-specific elements of sediment transport such as bedload and saltation. The effects of rainfall and surface runoff on discharge rates are not simulated directly within the model but are simplified and represented by variability in water depth within the irrigation channels. Studies have shown that rainfall increases can lead to an increase in surface runoff which in turn contribute to water flows in channels and canals, correspondingly increasing water depth (Linard, et al., 2009, Montgomery and Buffington, 1998) and resulting in higher water discharge rates. Erosive processes across the landscape are omitted and sediment inclusion is represented by the total suspended sediments in order to focus on sediments already present within the channels. The omission of erosive processes is because the presence of the stone-bound fields across the landscape would act to limit surface runoff and erosion (Mekonnen, et al., 2015, Lesschen, et al., 2009). In addition, the transport of sediments ties closely with the flow rate of water within the channels as the fast moving water will transport larger pebbles while slower flow rates would transport silt, sand and clay (Miedema, 2010, Sundborg, 1956). Studies by Lang and Stump

(2017) have shown that the sediments captured within the field system were predominantly clays which tend to be transported in suspension making bedload and saltation transport processes negligible for this model.

A.2 Model Parameterisation

Initial conditions for state variables in each grid cell (elevation in metres above sea level, soil-depth in metres, and angle of slope) are derived from DEMs, archaeological excavations and surveys of the study site. The initial values for the water discharge and sediment discharge vary among simulations; however, some baselines have been determined based on calibrations from existing data. Baselines such as water depth, used to determine cross sectional area of the channels, and total suspended sediments TSS, were based on data from hydrological studies conducted in 2015 along a 4 km stretch of the Engaruka River. The irrigation channel dimensions were based on archaeological measurements from studies conducted by Stump in 2003 in the North Fields of the Engaruka field system (Stump, 2006). The model parameters, their dimensions and default values are described in Table A. 1 below.

Table A.1: Model Parameters, variables and Initial values

Parameter	Explanation	Model initial/default value
Water Transport and Discharge		
Q	Water discharge (m^3s^{-1})	> 0
k	Dimensionless constant	1
n	Manning's roughness coefficient	0.03
R	Hydraulic radius (m)	> 0
S	The slope of the channel (m m^{-1}) i.e. the height difference between the start and end of the channel over the horizontal distance of the channel	0.02
A	Cross-sectional area of the channel (m^2)	> 0
<i>Canal dimensions</i>	Top width	1.0 m
	Bottom width	0.5 m
	Water depth	0.1 m
Sediment Transport and Discharge		
Q_s	Sediment discharge (tonnes day^{-1})	> 0
C_t	Daily total suspended sediment (mg L^{-1})	200

Parameter	Explanation	Model initial/default value
Y	Conversion factor that converts $\text{m}^3 \text{s}^{-1}$ to $\text{m}^3 \text{day}^{-1}$ and mg L^{-1} to tonnes m^{-3}	0.0864
Canal Networks		
CN_jQ	Transport and distribution of water discharge in the network of irrigation canals	> 0
CN_jQ_s	Transport and distribution of sediment discharge in the network of irrigation canals	> 0
w_l	Water discharge loss along the canal network	> 0
d_l	Sediment discharge loss along the network	> 0
t_w	Proportion of water discharge that continues to be transported along the canal networks (%)	0.80
t_d	Proportion of sediment discharge that continues to be transported along the canal networks (%)	0.85
r	Number of irrigation canal recipients in the network	> 0
Sediment Accumulation		
ΔH_i	Depositional layer thickness (m)	> 0
$\Delta S_{tot,i}$	Total sediment volume in a given stone-bound field i ($\text{m}^3 \text{day}^{-1}$)	> 0
f_i	Area of a given stone-bound field i (m^2)	36
$Q_{s,i}$	Sediment discharge within a given stone-bound field i (tonnes day^{-1})	> 0
BD	Bulk density of soils (1g cm^{-3} or 1000kg m^{-3})	1.10 – 1.60
C	Consolidation/compaction rate of soils (days)	365

699

700 A.3 ESTTraP Model ODD

701 A.3.1 ESTTraP Overview

702 Purpose

703 ESTTraP ABM was constructed to perform a series of simulations to understand the
704 temporal and spatial patterns for the transport and accumulation of sediments within
705 a section of the stone-bound fields in the Engarukan water-management system.

706 The purpose of this model is to understand the influence of irrigation infrastructure
707 and water diversion on the accumulation of sediments and development of a series
708 of stone-bound fields in the North fields of the historical irrigation system in
709 Engaruka, Tanzania. Sediment accumulation greatly influences field construction as
710 excavations by Stump (2006) show that as sediments accumulate the farmers place

additional drystone courses that over time raise their field walls. In this way, the development of the drystone fields is tied to sediment accumulation.

Engaruka North-fields Habitat entities, variables and scales

In this implementation of the model a block of 90 individual stone-bound fields, were modelled to understand the timescales and pattern of sediment accumulation given simulated scenarios of different environmental conditions. Each fields has a 6 × 6 m resolution, and the 90 field block covers approximately 3,000 m² of the 56,000 m² of the simulated landscape. The Engaruka North Fields habitat is characterised by state variables of topography and slope. The habitat is represented by field patches characterised by soil depth and elevation. The fields and irrigation canals are characterised by location and elevation data with the canals further characterised by water velocity generated from analysis of canal dimensions from archaeological excavations. The primary drivers of this model environment are water velocity and suspended sediment volumes within the canalised streams and irrigation canals. Initial conditions for the state variables are described in Appendix A.2 above.

Process overview and scheduling

The sediment deposition and accumulation process comprises four stages i.e. generation of water flows and sediments, water and sediment transport within the irrigation canals, sediment discharge in the fields and sediment accumulation over time. These processes occur within each year in the following order:

1. Water flows and sediment volumes are generated within the irrigation channels and modelled on the principles of continuous uniform open channel flows. The water flows and sediment volumes are distributed sequentially with the canalised stream receiving water first and then being distributed into the irrigation canals i.e. offtake canals and finally to the field offtake canals. In addition, the water distributed is divided amongst the total number of canalised stream and irrigation canals. In order to simulate water loss through seepage along the canalised stream and irrigation canals, a parameter of water loss is incorporated such that a certain proportion of the flows from the prior canal nodes are lost along the canals.
2. Water and sediments are transported within the irrigation canals with the water transporting suspended sediments. Similar to the water flows, some sediment

would be deposited along the water channels if the flows are not fast enough and do not reach the fields. In order to simulate this phenomenon, sediment loss along the canals was incorporated into the model.

3. Water and sediments are discharged into the fields from the irrigation canals.
4. Sediments that have been discharged accumulate over time in the fields; with sediment accumulation a function of sediment discharge and bulk density and the inverse of a soil consolidation factor for soil compaction over time.

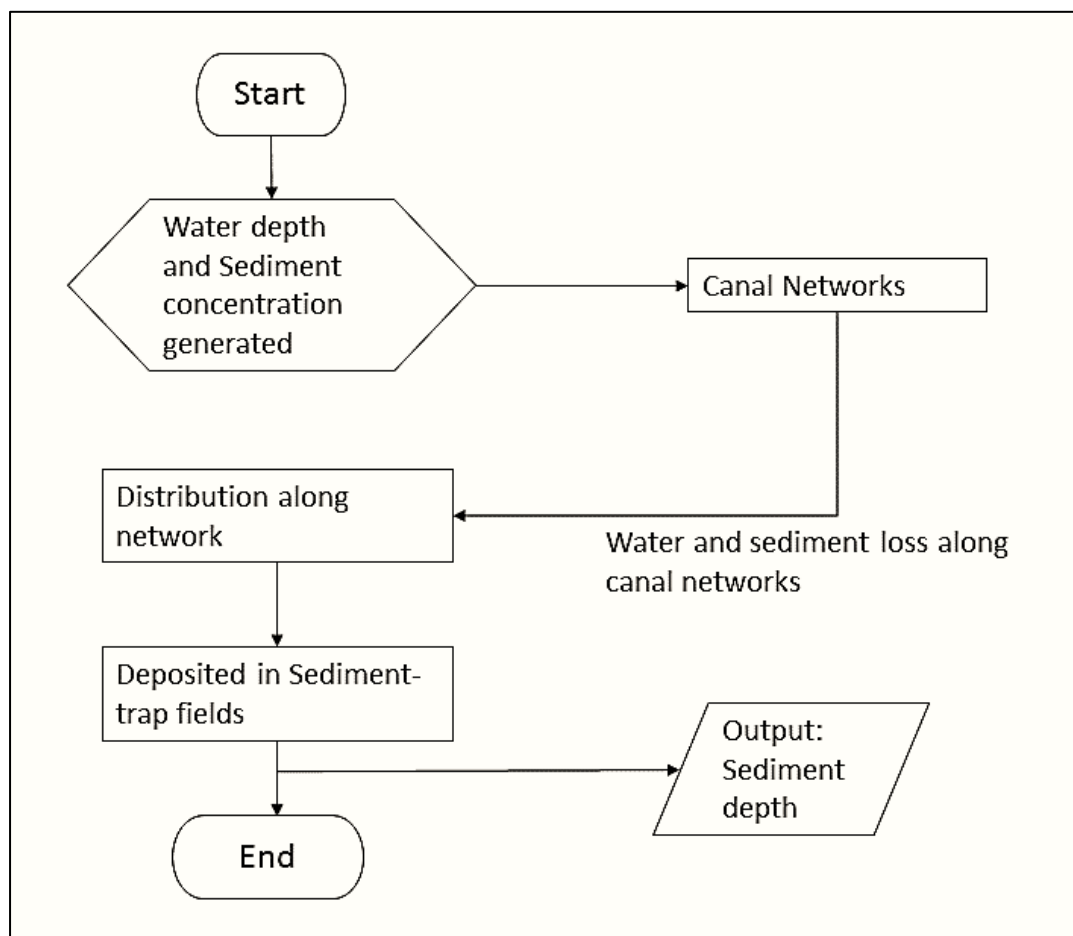


Figure A. 1: Flow diagram of the ESTTraP model processes

The total flows, sediment discharge and sediment depth for all the fields are collected at each time-step. The accumulation of sediments in the series of fields is calculated on a daily time-step and the results analysed to determine the amount of time required to accumulate the sediment depths that relate to the real world observations and archaeological observations.

A.3.2 ESTTraP Design concepts

Theoretical and Empirical background: The water flows, and sediment transport and deposition are modelled based on standard hydrological approaches including streamflow hydrology and sedimentation dynamics. The estimation of water discharge from the river channels and irrigation canals is based on the principles of open channel continuous flows for trapezoidal channels with Manning's roughness coefficient values within the range for natural streams with stone/pebble lined channels and excavated channels with rubble sides and earth bottom slope (Chow, 1959) . The sediment discharge is estimated from a sediment rating curve, which is a linear relationship of water discharge and total suspended sediments; while sedimentation processes are based on the principles of sediment accumulation (Robert, 2014, Wilkinson, et al., 2006, 7, Gordon, et al., 2004, van Rijn, 1984).

Individual decision-making: There is no individual decision-making.

Learning: There is no individual or collective learning included in the decision model. The agents do not change the decision-making rules.

Individual sensing: There is no individual sensing.

Individual prediction: The model makes no predictions.

Interactions: The rate of water discharge has an effect on the discharge of sediments, with a direct linear relationship between water and sediment discharge.

Collectives: The model contains no collectives.

Heterogeneity: There is no heterogeneity of decision-making by the agents.

Stochasticity: The amount of sediment discharged varies with changes in water discharge which is in turn influenced by the water height within the river channels and irrigation canals. In addition, the amount of water discharge decreases with increase in distance from the main canalised stream.

Observation: The amount of sediments deposited within the fields is collected on a daily time step. In addition, the water and sediment discharge from the canals is observed. The amount of sediment that accumulates within each stone-bound field is observed over time and the amount of water flows through the channels and canals is also noted. The amount of time it takes for a field to accumulate sediments of up to 700 mm in depth is recorded. The data is compared between the varied environmental scenarios of seasonal variability in water availability and erosive processes i.e. as represented by changes in water depth in the canalised stream and variations in suspended sediments, to determine the influence of these variations on the rates of sediments transported, deposited and accumulated within the fields. In addition the data is used for sensitivity analysis to assess the model's ability to produce results highlighting the implications of these scenarios on the influence of the water diversion infrastructure on field development and sediment accumulation within the irrigation system.

Emergence: The key results emerging from the model are patterns of sediment accumulation and field development over time, given the different environmental scenarios of water availability.

A.3.3 ESTTraP Details

Implementation Details

The model is implemented in Windows 7 using the NETLOGO platform version 5.2.1 (Wilensky, 1999). The hydrological and sediment-transport model is implemented through agents consisting of a network of nodes and directional links to represent the irrigation channels that transport water and sediments to the fields. The nodes contain information on the flow and sediment discharges along the system of canalised stream and irrigation channels based on the agent characteristics. The directed links that represent the irrigation channels distribute water and sediments from the canalised stream into the fields via nodes set within each 6 x 6 m field. At each time-step (representing the passage of one day) each node shares a percentage of its value of sediments and water equally with its neighbours in the network of nodes. The nodes also retain a percentage of the sediments and water flows to represent sediment and diffusion loss incurred as these agents move along the network. The transfer of sediments and water flows terminates at the fields,

where the nodes transfer these agents to the field patches as sediment discharge, which is then converted to represent sediment accumulation.

Initialisation

Initial conditions for state variables in each grid cell (elevation in metres above sea level, soil-depth in metres, and angle of slope) are derived from DEMs, archaeological excavations and surveys of the study site. The initial values for the water discharge and sediment discharge vary among simulations; however, some initial values have been determined based on existing data. Initial values such as water depth, used to determine cross sectional area of the channels and total suspended sediments (TSS), were based on data from hydrological studies conducted in 2015 along a 4 km² stretch of the Engaruka River. The irrigation channel dimensions were based on archaeological measurements from studies conducted by Stump in 2003 in the North Fields of the Engaruka field system (Stump, 2006). The model has four sub-models that represent the water and sediment discharge, irrigation canal networks and sediment accumulation. The model parameters, their dimensions and default values are described in Table A.1 above.

Input data

The elevation data for the model was obtained using a digital elevation model, the ASTER GDEM used is a product of METI and NASA (NASA_LP_DAAC, 2011). The input data for the model parameters, variables and initial values are outlined in Table A.1 above.

Submodels

The model runs on a daily time step with 365 steps per year, and with data collected at each time step on the amount of sediment accumulated and changes in sediment depth. The ESTTraP sub-models are described in Section 3 on material and methods of the manuscript.

Appendix B: Sensitivity and Uncertainty Analyses

B.1 Sensitivity and Uncertainty Analyses

Global sensitivity analysis of the model was conducted using the NetLogo BehaviorSpace and R 3.3.3 to explore the various model parameters in a systematic way. This was in order to explore the model behaviour for varying parameters and how they affect model outputs in order to see which parameters had the greatest influence on model outputs. The outputs were then graphically visualised in R using ggplot (Wickham, 2009) to assess the sensitivity of the model to variations in model inputs. The three main parameters of TSS, water depth in channels and Manning's roughness coefficient (n) have a great influence on the output variables under observation i.e. water and sediment discharge rates and the accumulation of sediments within the fields. Global sensitivity analysis was conducted where the selected input parameters for the model was run over all combinations of the main parameters and iterated for 365 time steps to represent a year.

Table B.1: Model parameters used for global sensitivity analysis in BehaviorSpace

Parameter	Min value	Max value	Varied by
Water depth	0.05	1.0	0.05
TSS	50	800	50
Manning's n	0.01	0.1	0.01

Exploratory global sensitivity analysis of the data shows that water and sediment discharge varied with water depth while sediment discharge also varied with TSS. As the water depth within the canalised streams and irrigation channels increased, the amount of sediment being discharged into the stone-bound fields increased even as the total suspended sediments were held constant (Figure B.1). This ties to existing literature that estimates suspended sediment discharge through the linear interpolation of estimated suspended sediment concentration and water discharge (Gray and Simões, 2008, 1066). The increase in sediment discharge can be related to the depth of the water column in the channels which allows for more water to flow through at a given time and thus transport more sediment. This means that even in instances where there is low sediment input from the surrounding catchment, possibly due to vegetation cover, variations in the water depth from increased water availability would influence the sediment discharge downstream. The water depth

and water discharge also affect sediment discharge particularly of fine sediments as these fine particles can be transported at low water discharge rates (Steegeen, et al., 2000, 31). This means that even in instances where water depth is low, sediment discharge of fine sediments will still occur. Therefore where fine sediments such as clay particles make up the majority of the total suspended sediment concentration, low water depths and slower water discharge rates can effectively transport sediments and the TSS volume becomes the predominant factor influencing sediment discharge (Figure B.1).

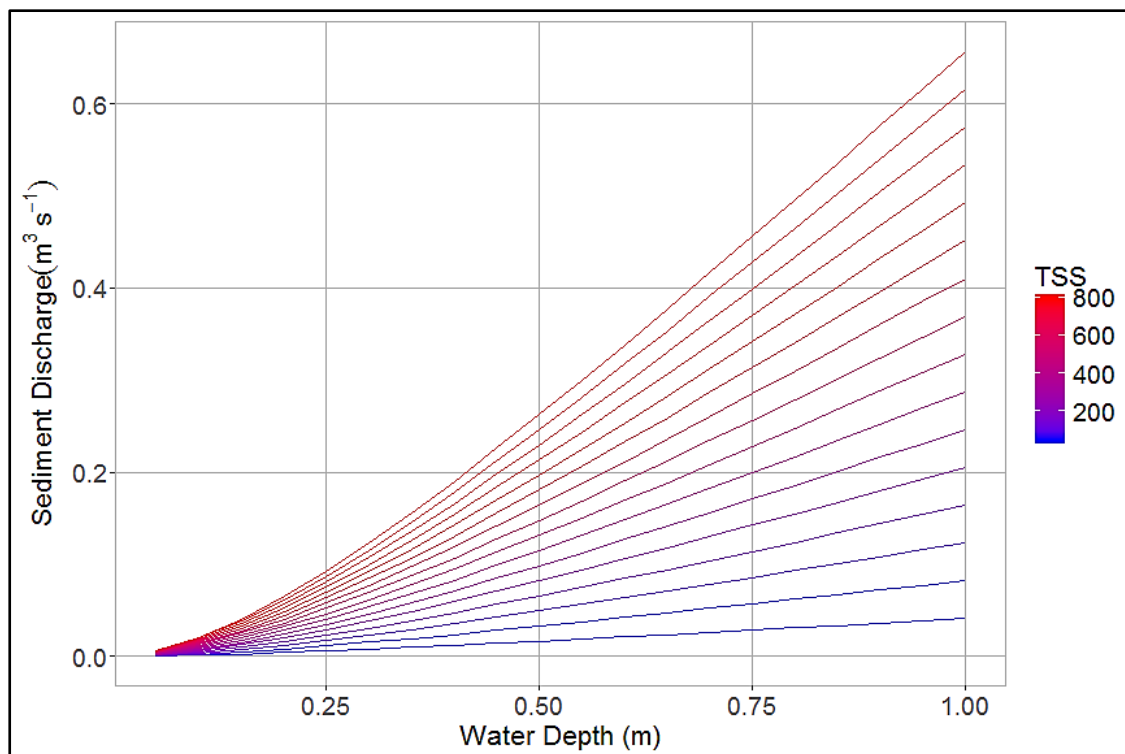


Figure B.1: Variations in mean annual sediment discharge ($\text{m}^3 \text{s}^{-1}$) with increasing water depth and total suspended sediment (mg L^{-1}) with Manning's n of 0.03

The sediment discharge also increased with increased suspended sediment volumes. Thus at a constant water depth increased TSS would result in increased sediment discharge. This is relevant in representing increased incorporation of sediments into the water channels during rain storm events and understanding the changes in sediment discharge between different seasons. Studies by Nu-Fang (2011) found that suspended sediment yield varied with the different seasons and was highest when water availability was greatest. The variability in TSS would therefore also affect the amount of sediment discharged and accumulated within the

field system. Since sediment discharge is a linear function of water and TSS, increase in the TSS values would therefore result in increase in the sediment discharged and therefore the accumulation rates in the fields. For the purposes of this model, a combination of variation in water depth and constant TSS would support representation of seasonal variations that would influence sediment accumulation as outlined below. Results of field studies conducted on water channels in the Engaruka found TSS values ranging from 50 to 800 mg/L, with the average TSS of 200 mg L⁻¹. The model therefore uses initial TSS values of 200 mg L⁻¹ and focuses on variability in water depth to simulate for the effects on water and sediment discharge.

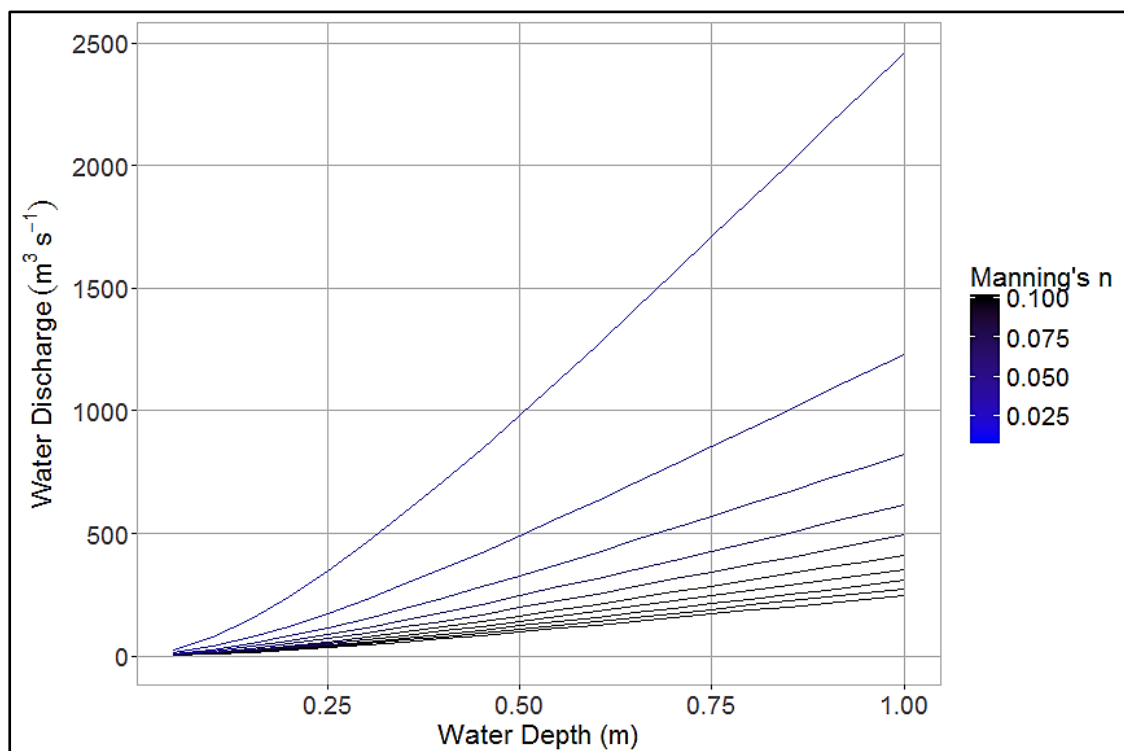


Figure B.2: Change in mean annual water discharge (m³ s⁻¹) with increasing water depth and changing Manning's roughness coefficient (n) values, with TSS of 200 mg L⁻¹

Water discharge was also found to vary with water depth and varying Manning's roughness coefficients (Figure B.2). An increase in the Manning's n resulted in a decrease in the water discharge while an increase in water depth in the channels resulted in an increase in water discharge across all Manning's n values. Low Manning's n values are typical of the surfaces of artificial channels made with materials intended to reduce friction while natural channel surfaces tend to have

931 higher roughness coefficients (Chow, 1959). Based on data from Stump (2006) from
932 excavations conducted in Engaruka, the water channels modelled can be described
933 as excavated or dredged, straight earth channels with earth bottoms and stone-lined
934 channel sides. The calibration for these channels can therefore be adjusted to
935 approximate n of 0.030 based on interpretation of Chow's (1959) reference
936 Manning's n values.

937 Increase in water depth resulted in increased water discharge (Figure B.2) and while
938 faster water discharge can seem useful in providing large supplies to fields, the high
939 water flows within the channels can result in damage to the channel walls by eroding
940 their surfaces. The preference would therefore be for lower water discharge at
941 channel water depths of less than 0.50 m. Calibration for other aspects of the cross-
942 sectional area of the channel i.e. bottom and top width and channel slope, were
943 based on the archaeological data from excavations conducted by Stump (2006). As
944 discussed above, sediment discharge can be interpolated from water discharge and
945 the model simulates the function as expected such that as water discharge increases
946 sediment discharge also increases.

947
948 Model Uncertainty analyses were conducted using NetLogo's BehaviorSpace where
949 the model scenario SIM-01 was run 100 times before stratified random sampling was
950 used to extract 100 random variables from the runs. These 100 runs were then
951 analysed using descriptive statistics in Excel to generate univariate statistics on the
952 variability and the central tendency of the sample group (Figure B.3).

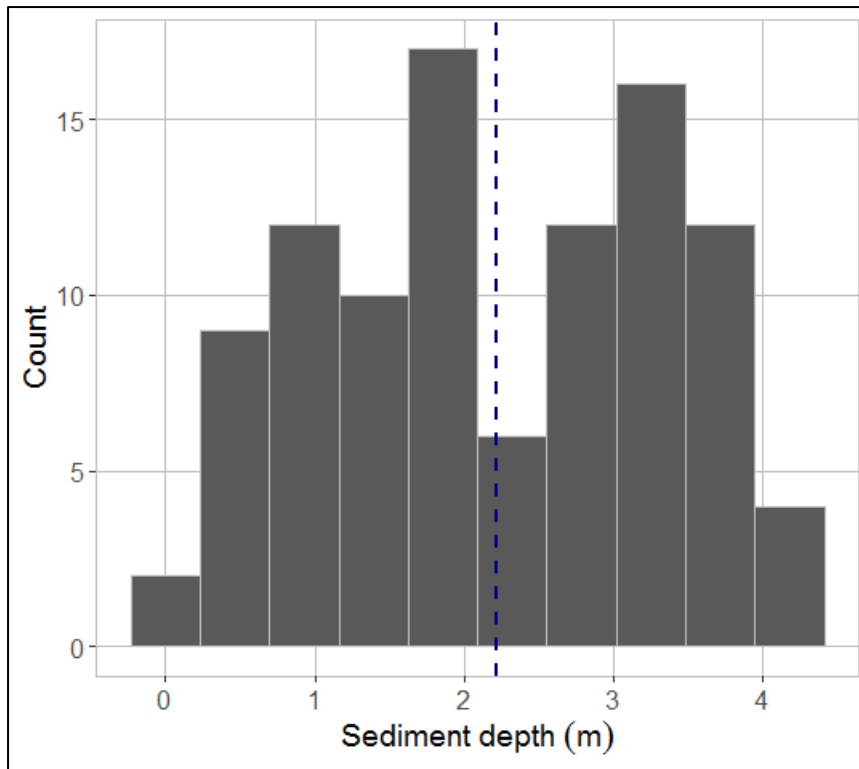


Figure B.3: Histogram of 100 replicates displaying distribution of sediment depths for model outputs for SIM-01 scenario indicating the mean (blue dashed line).

The summary statistics and histogram show that the data has a bimodal distribution with a mean of 2.21 m, standard deviation 1.14, sample variance of 1.30 and confidence level (95%) of 0.23. The peaks for the data fall within the range of the first quartile at 1.38m and the third quartile at 3.28m. This bimodality in the distribution of data can be due to selection of random variables from the data at different points in the time period as the model ran.

B.2 Equivalence of Tested Scenarios

The scenarios simulated utilised changes in water depth as proxies for the seasonal and long-term climate fluctuations that could affect water availability and thus water depth. The average daily water-depth for each scenario was determined where in SIM-01 average water-depth was 0.10 m per day, for SIM-02 the average daily water depth was 0.073 m, for SIM-03 the average daily water depth was 0.064 m, and for SIM-04 the average daily water depth was 0.093 m. This brings the question of whether the results of the scenarios simulated were due to the differences in average daily water depth or due to the trends in water depth over time. In order to

determine this the scenarios were also run with seasonal and long-term fluctuations where water-depth would vary over different seasons but would still result in an average daily water depth of 0.10 m overall in order to assess the equivalence of the tested scenarios (Fig B.3).

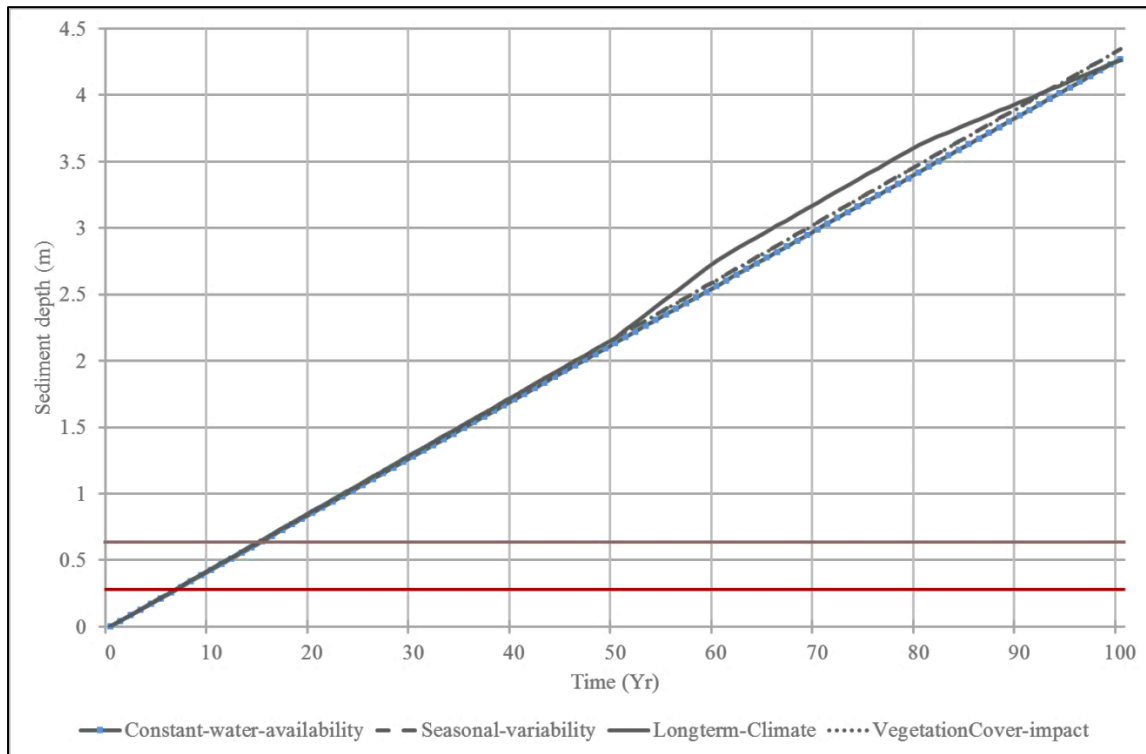


Figure B.4: Mean annual cumulative sediment depth (metres) for constant water availability (SIM-01), seasonal variability (SIM-02), long-term climate variability (SIM-03), and vegetation cover impact (SIM-04) over a period of 100 years.

The results of the equivalence test showed that when the average daily water depth was the same between the scenarios with different trends over time, the rates of sediment accumulation closely matched. However it must be noted that in realistic depictions of water availability, the seasonal and climate fluctuations mean that there might be less water available in the water channels to transport water and sediments to the fields thus these two variables are interlinked. The changes in water depth due to differences in trends of water distribution as a result of seasonal and long-term climate fluctuations would result in averaged daily water depths being lower than the idealised rate, it would thus mean that it would be the combination of trends in water distribution over time and the differences in water availability that would influence the rate of sediment accumulation in the fields.

996

997 **Acknowledgements**

998 The Archaeology of Agricultural Resilience in Eastern Africa (AAREA) project is
999 funded by the European Research Council under the European Union's Seventh
1000 Framework Programme Starter Grant Scheme (FP/200702013/ERC); Grant
1001 Agreement No. ERC-StG-2012-337128-AAREA was awarded to D. Stump in
1002 February 2014. The research was also supported by funding awarded by the British
1003 Institute in East Africa to T.K. Kabora under the Thematic Research Grants
1004 2015/2016. The research in Tanzania was carried out under a research permit
1005 issued by the Tanzanian Commission for Science and Technology and an
1006 excavation license issued by the Antiquities Unit of the Ministry of Natural Resources
1007 and Tourism. The help and support provided by both these agencies is gratefully
1008 acknowledged. The authors would like to thank the anonymous peer reviewers for
1009 their comments and critiques that helped improve this paper, and in particular the
1010 authors would like to thank Iza Romanowska for taking the time to review the model
1011 code.

1012

1013 **References**

- 1014 Mekonnen, M., Keesstra, S.D., Stroosnijder, L., Baartman, J.E.M., Maroulis, J.,
1015 2015. Soil Conservation Through Sediment Trapping: A Review, *Land Degradation &*
1016 *Development* 26, 544-556.
- 1017 Beckers, B., Berking, J., Schütt, B., 2013. Ancient water harvesting methods in the
1018 drylands of the Mediterranean and Western Asia, *eTopoi. Journal for Ancient*
1019 *Studies*.
- 1020 Ferro-Vázquez, C., Lang, C., Kaal, J., Stump, D., 2017. When is a terrace not a
1021 terrace? The importance of understanding landscape evolution in studies of terraced
1022 agriculture, *Journal of Environmental Management* 202, 500-513.
- 1023 Hill, J., Woodland, W., 2003. Contrasting water management techniques in Tunisia:
1024 towards sustainable agricultural use, *The Geographical Journal* 169, 342-357.

- 1025 Giráldez, J.V., Ayuso, J.L., Garcia, A., López, J.G., Roldán, J., 1988. Water
1026 harvesting strategies in the semiarid climate of southeastern Spain, *Agricultural*
1027 *Water Management* 14, 253-263.
- 1028 Abedini, M., Md Said, M.A., Ahmad, F., 2012. Effectiveness of check dam to control
1029 soil erosion in a tropical catchment (The Ulu Kinta Basin), *CATENA* 97, 63-70.
- 1030 Ran, D.-C., Luo, Q.-H., Zhou, Z.-H., Wang, G.-Q., Zhang, X.-H., 2008. Sediment
1031 retention by check dams in the Hekouzhen-Longmen Section of the Yellow River,
1032 *International Journal of Sediment Research* 23, 159-166.
- 1033 Fisher, C., 2019. Archaeology for Sustainable Agriculture, *Journal of Archaeological*
1034 *Research*.
- 1035 Logan, A.L., Stump, D., Goldstein, S.T., Orijemie, E.A., Schoeman, M.H., 2019.
1036 Usable Pasts Forum: Critically Engaging Food Security, *Afr Archaeol Rev* 36, 419-
1037 438.
- 1038 Evenari, M., Shanan, L., Tadmor, N., 1982. *The Negev: the challenge of a desert*,
1039 Harvard University Press.
- 1040 Morrison, K.D., 2015. Archaeologies of flow: Water and the landscapes of Southern
1041 India past, present, and future, *Journal of Field Archaeology* 40, 560-580.
- 1042 Sheridan, M.J., 2002. An Irrigation Intake Is like a Uterus: Culture and Agriculture in
1043 Precolonial North Pare, Tanzania, *American Anthropologist* 104, 79-92.
- 1044 Stump, D., 2016. Digging for Indigenous Knowledge: 'Reverse Engineering' and
1045 Stratigraphic Sequencing as a Potential Archaeological Contribution to Sustainability
1046 Assessments, in: Isendahl, C., Stump, D. (Eds.), *The Oxford Handbook of Historical*
1047 *Ecology and Applied Archaeology*, Oxford University Press, Oxford Handbooks
1048 Online.
- 1049 Stump, D., 2006. The development and expansion of the field and irrigation systems
1050 at Engaruka, Tanzania, *AZANIA: Journal of the British Institute in Eastern Africa* 41,
1051 69-94.

- 1052 Lang, C., Stump, D., 2017. Geoarchaeological evidence for the construction,
1053 irrigation, cultivation, and resilience of 15th--18th century AD terraced landscape at
1054 Engaruka, Tanzania, *Quaternary Research*, 1-18.
- 1055 Ryner, M., Holmgren, K., Taylor, D., 2008. A record of vegetation dynamics and lake
1056 level changes from Lake Emakat, northern Tanzania, during the last c. 1200 years, *J*
1057 *Paleolimnol* 40, 583-601.
- 1058 Verschuren, D., Laird, K.R., Cumming, B.F., 2000. Rainfall and drought in equatorial
1059 east Africa during the past 1,100 years, *Nature* 403, 410-414.
- 1060 Ding, Z., Gong, W., Li, S., wu, Z., 2018. System Dynamics versus Agent-Based
1061 Modeling: A Review of Complexity Simulation in Construction Waste Management,
1062 *Sustainability* 10, 2484.
- 1063 Martin, R., Schlüter, M., 2015. Combining system dynamics and agent-based
1064 modeling to analyze social-ecological interactions—an example from modeling
1065 restoration of a shallow lake, *Frontiers in Environmental Science* 3.
- 1066 Siebers, P.O., Macal, C.M., Garnett, J., Buxton, D., Pidd, M., 2010. Discrete-event
1067 simulation is dead, long live agent-based simulation!, *J. Simul.* 4, 204-210.
- 1068 Bonabeau, E., 2002. Agent-based modeling: Methods and techniques for simulating
1069 human systems, *Proceedings of the National Academy of Sciences* 99, 7280-7287.
- 1070 Barton, M.C., 2016. From Narratives to Algorithms: Extending Archaeological
1071 Explanation beyond Archaeology, in: Isendahl, C., Stump, D. (Eds.), *The Oxford*
1072 *Handbook of Historical Ecology and Applied Archaeology*, Oxford University Press,
1073 Oxford Handbooks Online.
- 1074 Westerberg, L.-O., Holmgren, K., BÖrjeson, L., HÅkansson, N.T., Laulumaa, V.,
1075 Ryner, M., Öberg, H., 2010. The development of the ancient irrigation system at
1076 Engaruka, northern Tanzania: physical and societal factors, *Geographical Journal*
1077 176, 304-318.
- 1078 Sutton, J.E.G., 1978. Engaruka and its Waters, *Azania: Archaeological Research in*
1079 *Africa* 13, 37-70.

- 1080 Sutton, J.E.G., 1998. Engaruka: An Irrigation Agricultural Community in Northern
1081 Tanzania Before the Maasai, *Azania: Journal of the British Institute in Eastern Africa*
1082 33, 1-37.
- 1083 Laulumaa, V., 2006. Estimation of the population of ancient Engaruka—a new
1084 approach, *Azania: Archaeological Research in Africa* 41, 95-102.
- 1085 Esri, 2011. National Geographic [basemap]. Scale 1:144,000. National Geographic
1086 World Map. 13 December 2011.
1087 <http://www.arcgis.com/home/item.html?id=b9b1b422198944fbbd5250b3241691b6>.
1088 (15 February 2017).
- 1089 Doolittle, W.E., 2015. Expedience, Impermanence, and Unplanned
1090 Obsolescence The Coming-About of Agricultural Features and Landscapes, in:
1091 Isendahl, C., Stump, D., Doolittle, W.E. (Eds.), *The Oxford Handbook of Historical*
1092 *Ecology and Applied Archaeology*, Oxford University Press.
- 1093 Howard, J.B., 1993. A paleohydraulic approach to examining agricultural
1094 intensification in Hohokam irrigation systems. In Scarborough, V.L. and B.L. Isaac
1095 (eds.) *Economic Aspects of Water Management in the Prehispanic New World.*,
1096 *Research in Economic Anthropology Supplement* 7, 263-324.
- 1097 Doolittle, W.E., 1984. Agricultural Change as an Incremental Process, *Annals of the*
1098 *Association of American Geographers* 74, 124-137.
- 1099 Wilensky, U., 1999. NetLogo. <http://ccl.northwestern.edu/netlogo/>. Center for
1100 Connected Learning and Computer-Based Modeling, Northwestern University,
1101 Evanston, IL.
- 1102 Müller, B., Bohn, F., Dreßler, G., Groeneveld, J., Klassert, C., Martin, R., Schlüter,
1103 M., Schulze, J., Weise, H., Schwarz, N., 2013. Describing human decisions in agent-
1104 based models – ODD + D, an extension of the ODD protocol, *Environmental*
1105 *Modelling & Software* 48, 37-48.
- 1106 Grimm, V., Berger, U., Bastiansen, F., Eliassen, S., Ginot, V., Giske, J., Goss-
1107 Custard, J., Grand, T., Heinz, S.K., Huse, G., Huth, A., Jepsen, J.U., Jørgensen, C.,
1108 Mooij, W.M., Müller, B., Pe'er, G., Piou, C., Railsback, S.F., Robbins, A.M., Robbins,

1109 M.M., Rossmanith, E., Rüger, N., Strand, E., Souissi, S., Stillman, R.A., Vabø, R.,
 1110 Visser, U., DeAngelis, D.L., 2006. A standard protocol for describing individual-
 1111 based and agent-based models, *Ecol. Model.* 198, 115-126.

1112 NASA_LP_DAAC, 2011. ASTER Global Digital Elevation Model (GDEM) 1 arc
 1113 second. Version 2. 03°S, 35°E. , NASA EOSDIS Land Processes Distributed Active
 1114 Archive Center (LP DAAC), USGS Earth Resources Observation and Science
 1115 (EROS) Center, Sioux Falls, South Dakota. [DOI:
 1116 <http://dx.doi.org/10.5067/ASTER/ASTGTM.002>]

1117 Robert, A., 2014. River processes: an introduction to fluvial dynamics, Routledge.

1118 Van Rijn, L.C., 1993. Principles of sediment transport in rivers, estuaries and coastal
 1119 seas, Aqua publications Amsterdam.

1120 van Rijn, L.C., 2013. Sedimentation of Sand and Mud in Reservoirs in Rivers.

1121 Wilkinson, S.N., Prosser, I.P., Hughes, A.O., 2006. Predicting the distribution of bed
 1122 material accumulation using river network sediment budgets, *Water Resources*
 1123 *Research* 42, n/a-n/a.

1124 McKenzie, N., Coughlan, K., Cresswell, H., 2002. Soil physical measurement and
 1125 interpretation for land evaluation, Csiro Publishing.

1126 FAO, 2006. Guidelines for Soil Description., 4 ed., Food and Agriculture
 1127 Organization of the United Nations, Rome.

1128 Harris, I., Jones, P.D., Osborn, T.J., Lister, D.H., 2014. Updated high-resolution grids
 1129 of monthly climatic observations – the CRU TS3.10 Dataset, *International Journal of*
 1130 *Climatology* 34, 623-642.

1131 Thiele, J.C., Kurth, W., Grimm, V., 2014. Facilitating Parameter Estimation and
 1132 Sensitivity Analysis of Agent-Based Models: A Cookbook Using NetLogo and 'R',
 1133 *Journal of Artificial Societies and Social Simulation* 17, 11.

1134 Saltelli, A., Ratto, M., Andres, T., Campolongo, F., Cariboni, J., Gatelli, D., Saisana,
 1135 M., Tarantola, S., 2008. Global sensitivity analysis: the primer, John Wiley & Sons.

1136 Seidel, M., Hlawitschka, M., 2015. An R-Based Function for Modeling of End
1137 Member Compositions, *Mathematical Geosciences* 47, 995-1007.

1138 Jones, P., Harris, I., 2008. Climatic Research Unit (CRU) time-series datasets of
1139 variations in climate with variations in other phenomena, NCAS British Atmospheric
1140 Data Centre.

1141 Marchant, R., Richer, S., Boles, O., Capitani, C., Courtney-Mustaphi, C.J., Lane, P.,
1142 Prendergast, M.E., Stump, D., De Cort, G., Kaplan, J.O., Phelps, L., Kay, A., Olago,
1143 D., Petek, N., Platt, P.J., Punwong, P., Widgren, M., Wynne-Jones, S., Ferro-
1144 Vázquez, C., Benard, J., Boivin, N., Crowther, A., Cuní-Sánchez, A., Deere, N.J.,
1145 Ekblom, A., Farmer, J., Finch, J., Fuller, D., Gaillard-Lemdl, M.-J., Gillson, L.,
1146 Githumbi, E., Kabora, T., Kariuki, R., Kinyanjui, R., Kyazike, E., Lang, C., Lejju, J.,
1147 Morrison, K.D., Muiruri, V., Mumbi, C., Muthoni, R., Muzuka, A., Ndiema, E., Kabonyi
1148 Nzabandora, C., Onjala, I., Schrijver, A.P., Rucina, S., Shoemaker, A., Thornton-
1149 Barnett, S., van der Plas, G., Watson, E.E., Williamson, D., Wright, D., 2018. Drivers
1150 and trajectories of land cover change in East Africa: Human and environmental
1151 interactions from 6000 years ago to present, *Earth-Science Reviews* 178, 322-378.

1152 Barker, P., Gasse, F., 2003. New evidence for a reduced water balance in East
1153 Africa during the Last Glacial Maximum: implication for model-data comparison,
1154 *Quaternary Science Reviews* 22, 823-837.

1155 Lesschen, J.P., Schoorl, J.M., Cammeraat, L., 2009. Modelling runoff and erosion for
1156 a semi-arid catchment using a multi-scale approach based on hydrological
1157 connectivity, *Geomorphology* 109, 174-183.

1158 Wainwright, J., 2008. Can modelling enable us to understand the rôle of humans in
1159 landscape evolution?, *Geoforum* 39, 659-674.

1160 Linard, J.I., Wolock, D.M., Webb, R.M., Wiecezorek, M.E., 2009. Identifying hydrologic
1161 processes in agricultural watersheds using precipitation-runoff models, US
1162 Geological Survey.

1163 Montgomery, D.R., Buffington, J.M., 1998. Channel processes, classification, and
 1164 response, in: Naiman, R.J., Bilby, R.E. (Eds.), *River Ecology and Management: Lessons from the Pacific Coastal Ecoregion*, Springer, New York, pp. 13 - 42.

1166 Miedema, S., 2010. Constructing the Shields curve, a new theoretical approach and
 1167 its applications, WODCON XIX, Beijing China.

1168 Sundborg, Å., 1956. The River Klarälven: A Study of Fluvial Processes, *Geografiska Annaler* 38, 125-237.

1170 Chow, T.V., 1959. *Open-channel hydraulics*, McGraw-Hill.

1171 Gordon, N.D., McMahon, T.A., Finlayson, B.L., 2004. *Stream hydrology: an introduction for ecologists*, John Wiley and Sons.

1173 van Rijn, L.C., 1984. Sediment Transport 2: Suspended load transport, *J. Hydraul. Eng.-ASCE* 110, 1613-1641.

1175 Wickham, H., 2009. *ggplot2: Elegant Graphics for Data Analysis*, Springer-Verlag New York.

1177 Gray, J.R., Simões, F.J., 2008. Estimating sediment discharge, *Sedimentation Engineering: Processes, Measurements, Modeling, and Practice*, pp. 1067-1088.

1179 Steegen, A., Govers, G., Nachtergaele, J., Takken, I., Beuselinck, L., Poesen, J., 2000. Sediment export by water from an agricultural catchment in the Loam Belt of central Belgium, *Geomorphology* 33, 25-36.

1182 Nu-Fang, F., Zhi-Hua, S., Lu, L., Cheng, J., 2011. Rainfall, runoff, and suspended sediment delivery relationships in a small agricultural watershed of the Three Gorges area, China, *Geomorphology* 135, 158-166.

1185